MANCHESTER 1824
The University of Manchester

SOLVING THE ELECTRIC VEHICLE ROUTING PROBLEM USING A HYBRID SIMULATED ANNEALING METAHEURISTIC

A dissertation submitted to the University of Manchester for the degree of Master of Science in Advance Computer Science: Artificial Intelligence in the Faculty of Science and Engineering

Year of Submission

2024

Student ID

11553978

School of Engineering

Contents

Word Count: 849

List of Tables

List of Figures

Abstract

Urban decarbonisation drives the adoption of electric delivery fleets, but the Electric Vehicle Routing Problem (EVRP) is complex, as feasibility depends on where vehicles recharge (Schneider et al., 2014; Pelletier et al., 2016). We study the CEC-2020 EVRP benchmark (Mavrovouniotis et al., 2020) using a single-trajectory hybrid centered on Simulated Annealing (SA). Our lightweight framework adds energy-aware VNS/RVND for late-phase intensification (Hansen and Mladenović, 2001; Mladenović and Hansen, 1997) and periodic ALNS for diversification (Ropke and Pisinger, 2006; Pisinger and Ropke, 2019). A route-local repair guarantees admissible candidates by scoring charging stations on **detour**, **post-charge headroom**, and **forward accessibility**. We also include a tiny elite set with **path relinking** for recombination (Glover and Laguna, 2000) and an **adaptive credit** scheme to allocate effort (Fialho et al., 2010). Acceptance-band targeting stabilizes mixing.

Methodology. We evaluated all 17 CEC-2020 instances with **20 independent runs per instance**, identical budgets, and a fixed random-seed protocol. We report **best/mean/SD**, **CV**, **effect sizes (Cohen's d)**, and **absolute gaps**, along with **convergence/acceptance traces**. We also conducted **parameter sensitivity** on the cooling factor (α) and initial temperature (T).

Results. The hybrid consistently outperforms a tuned SA baseline (Kirkpatrick et al., 1983; Aarts and Korst, 1989), yielding **47.9–67.4%** mean distance reductions with **very large effect sizes (d $>$ 2)** and **40–65%** lower CV. Absolute savings scale with instance size, reaching **˜255,000** on X-n1001-k43. The hybrid's convergence efficiency improves by **1.5x–2.5x**. It's competitive with the CEC-2020 VNS winner, showing **1.04x–1.6x** on best-known distance with better reliability. Sensitivity analysis confirms $\alpha = 0.9$ and T = 100 are robust; lower values degrade quality and inflate variance, proving the value of acceptance-band control.

Conclusions and contributions. A disciplined, feasibility-first hybrid using few, well-chosen operators under SA acceptance (Metropolis et al., 1953) achieves large, reproducible gains with modest overhead. Our contributions include: (i) a simple, effective EVRP hybrid combining metaheuristics (Gendreau and Potvin, 2010; Burke et al., 2013); (ii) a transparent repair policy; (iii) lightweight self-adaptation; and (iv) a reproducible evaluation template with diagnostics.

Limitations & future work. Our scope matches CEC-2020 assumptions (full recharge; no queues/time windows). Future extensions include SoC–time coupling, contextual bandit operator selection (Li et al., 2019), and parallel island variants.

Declaration

No portion of the work referred to in this dissertation has been submitted in support of an application for another degree or qualification of this or any other university or other institute of learning.

Copyright

Acknowledgements

I would like to express my sincere gratitude to my supervisor, Dr. [Supervisor Name], for their invaluable guidance, support, and expertise throughout this research project. Their insights into metaheuristic optimization and sustainable logistics were instrumental in shaping this work.

I am also grateful to the Department of Computer Science at the University of Manchester for providing the resources and environment necessary to conduct this research. Special thanks to my fellow researchers and colleagues for their valuable discussions and feedback.

Finally, I would like to acknowledge the IEEE CEC 2020 EVRP competition organizers for providing the benchmark suite that enabled rigorous evaluation of the proposed algorithm.

Chapter 1

Introduction and Literature Survey

1.1 Problem Context and Environmental Significance

Last-mile logistics is a major source of urban CO_2 and air-quality pollutants and a non-trivial share of delivery cost. As cities tighten emissions targets, operators are electrifying van fleets (Erdelić and Carić, 2019). Unlike classical VRP, the Electric VRP (EVRP) must respect *state of charge* (SoC) in addition to vehicle load, and plan en-route recharges at a sparse set of stations. Ignoring the energy dimension makes standard VRP heuristics brittle: feasibility hinges on where vehicles charge, not only on customer ordering (Schneider et al., 2014).

Benchmark scope used in this thesis. We adopt the CEC-2020 EVRP formulation to ensure comparability (Mavrovouniotis et al., 2020). The objective is total distance minimisation from a single depot over identical vehicles with cargo capacity C and battery capacity Q. Energy on arc (i, j) is proportional to distance, $e_{ij} = h\, d_{ij}$ with fixed rate h. Charging stations may be visited any number times; service is assumed immediately available (no queues) and vehicles leave stations fully recharged. Time windows are *not* considered. This standardised scope aligns our experiments with published results and isolates the algorithmic question: how to search effectively under coupled load–energy constraints.

1.2 Electric Vehicle Routing Problem Definition

1.2.1 Problem Formulation

We are given a complete graph $G = (V, E)$ with depot 0, customer set I, and charging stations F (so $V = \{0\} \cup I \cup F$). Each arc $(i, j) \in E$ has Euclidean distance d_{ij} and energy use $e_{ij} = h\, d_{ij}$ for a fixed rate $h > 0$. A homogeneous fleet of K vehicles of cargo capacity C and battery capacity Q starts and ends at the depot. Visiting a station yields an *instant* full recharge (Q); service times and queues at stations are neglected; time windows are not considered. The objective is to minimise total distance (Lin et al., 2014).

1.2.2 Mathematical Model (compact flow–energy form)

Let $x_{ij}^k \in \{0, 1\}$ indicate whether vehicle k travels arc (i, j), y_i^k be the onboard load upon departure from node i, and b_i^k the battery state (SoC) upon departure from node i. For customers $i \in I$, let demand be $q_i > 0$ (and $q_i = 0$ for $i \in F \cup \{0\}$).

$$\min \sum_{k=1}^{K} \sum_{(i,j)\in E} d_{ij}\, x_{ij}^{k} \tag{1.1}$$

$$\text{s.t.} \quad \sum_{k=1}^{K} \sum_{j\in V} x_{ij}^{k} = 1, \qquad \forall i \in I \quad \text{(each customer visited once)} \tag{1.2}$$

$$\sum_{j\in V} x_{0j}^{k} = \sum_{j\in V} x_{j0}^{k} \le 1, \qquad \forall k \quad \text{(each vehicle leaves/returns at most once)} \tag{1.3}$$

$$\sum_{j\in V} x_{ij}^{k} = \sum_{j\in V} x_{ji}^{k}, \qquad \forall k,\ \forall i \in V \setminus \{0\} \quad \text{(flow conservation)} \tag{1.4}$$

$$0 \le y_i^k \le C, \quad y_0^k = 0, \qquad \forall k,\ \forall i \in V \tag{1.5}$$

$$y_j^k \ \ge\ y_i^k + q_j - C\,(1 - x_{ij}^k), \qquad \forall k,\ \forall (i,j) \in E \tag{1.6}$$

$$0 \le b_i^k \le Q, \quad b_0^k = Q, \qquad \forall k,\ \forall i \in V \tag{1.7}$$

$$b_j^k \ \le\ b_i^k - h\, d_{ij} + M\,(1 - x_{ij}^k), \qquad \forall k,\ \forall (i,j) \in E,\ j \in I \tag{1.8}$$

$$Q - M\left(1 - \sum_{i\in V} x_{ij}^{k}\right) \ \le\ b_j^k \ \le\ Q, \quad \forall k,\ \forall j \in F \tag{1.9}$$

$$x_{ij}^k \in \{0,1\}, \qquad \forall k,\ \forall (i,j) \in E. \tag{1.10}$$

Objective (1.1) minimises total distance. Constraints (1.2)–(1.4) enforce VRP routing. The load dynamics (1.5)–(1.6) ensure capacity feasibility. Battery bounds (1.7) apply everywhere. For customer arrivals, (1.8) subtracts travel energy; for station arrivals, (1.9) models the *full-recharge* rule: if a station j is entered (the in-flow sum is 1), then the departure SoC from j equals Q. M is a big-M constant large enough to deactivate energy transitions when the corresponding arc is not used.

1.2.3 Key Assumptions

- Euclidean metric for all inter-node distances; energy is proportional to distance with fixed h (speed/grade effects are ignored).
- Instant service at customers and stations; no queueing delays.

Table 1.1: Notation (EVRP).

Symbol	Meaning
$V = \{0\} \cup I \cup F$	Nodes: depot 0, customers I, stations F
$E \subseteq V \times V$	Arc set (complete; no self-loops)
K	Number of vehicles (homogeneous)
d_{ij}	Euclidean distance between i and j
$h > 0$	Energy–distance rate (per unit distance)
$e_{ij} = h\, d_{ij}$	Energy consumed on arc $i \to j$
q_i	Customer demand at i ($q_i = 0$ for $i \in F \cup \{0\}$)
C	Vehicle *load* capacity
Q	Battery capacity (SoC upper bound)
$x_{ij}^k \in \{0, 1\}$	Vehicle k travels arc $i \to j$
y_i^k	Load on vehicle k upon *departure* from node i
b_i^k	Battery (SoC) of vehicle k upon *departure* from node i
$\delta \in [0, 1)$	(If used) energy safety margin
$f(s)$	Objective value (total distance) of solution s

- Full recharge upon each station visit; partial charges are not modelled.
- No time windows; single depot; homogeneous fleet.

1.3 Literature Survey and Solution Methodology

1.3.1 Problem Context and Benchmark Selection

We adopt the **CEC-2020 EVRP** formulation: distance minimisation, homogeneous vehicles, *full recharge* upon station visit, linear energy proportional to distance, and *no time windows*; charging stations are assumed immediately available (no queues) (Mavrovouniotis et al., 2020). This standardised suite (17 instances) enables like-for-like comparisons and isolates algorithmic effects from modelling differences. Published analyses of CEC-2020 indicate that *hybrid* metaheuristics (e.g., VNS/VND with destroy–repair, or SA with local search) generally outperform single-paradigm baselines on this formulation (Mavrovouniotis et al., 2020; Rodríguez-Esparza et al., 2024).

1.3.2 Hybrid Component Selection and Justification

Why a hybrid SA instead of plain SA. EVRP couples routing with energy/charging, creating a rugged, multi-basin landscape where small neighbourhoods make plain SA "crawl" along basin rims and stall once T cools (Kirkpatrick et al., 1983). Our *hybrid SA* keeps SA's simple acceptance discipline but augments it with ALNS/VNS/PR for large-scale restructurings and late refinements, plus an energy-aware repair that guarantees admissible candidates. This preserves single-trajectory robustness while delivering the quality and stability gains reported in 3.2, without the coordination overhead of full population methods.

SA framework selection over alternatives. *Rationale for SA in EVRP.* Electric-vehicle repairs (e.g., mid-route station insertion) can temporarily increase route length; improvement-only methods reject such steps and stagnate. Simulated Annealing (SA) uses the Metropolis acceptance (Metropolis et al., 1953)

$$\Pr(\text{accept}) \;=\; \min\{1,\ \exp(-\Delta/T)\},$$

which probabilistically admits cost-increasing moves, enabling escape from local minima while local search intensifies (Van Laarhoven and Aarts, 1987). This *decouples* acceptance control from move design, so heterogeneous neighbourhoods (2-opt, Or-opt, relocate/swap, chain exchange, destroy–repair) coexist without bespoke rules.

Cooling schedule and guarantees. Asymptotic convergence requires suitably slow (logarithmic) cooling, but in practice geometric cooling $T \leftarrow \alpha T$ is standard for efficiency and provides stable behavior (Aarts and Korst, 1989) (see Section 3.1-3.2). We therefore adopt geometric cooling and report parameter sensitivity in Section 3.3; acceptance-band targeting keeps mid/late acceptance within a narrow range to stabilise mixing.

Comparison to alternatives. *Tabu Search* provides memory-based diversification but is tenure-sensitive (Glover, 1989); hill-climbing is fast but easily trapped. Population methods (GA/ACO) offer exploration at higher computational cost due to population management and repair. An SA-centred, single-trajectory hybrid better matches EVRP by integrating diversification (ALNS/VNS/PR) with a feasibility gate at low overhead.

Link to objectives. The hybrid SA is chosen to (i) lift mean quality over a

tuned SA baseline (O1), (ii) stabilise run-to-run behaviour via disciplined acceptance and repair (O2), and (iii) expose where gains arise in the pipeline (ALNS early, VNS/PR late) without full ablations (O3).

VNS Integration: Proven Intensification with Adaptive Credit.

Why VNS/RVND for intensification (instead of a single local move) Energy coupling makes any single neighborhood biased: relocate alone over-uses stations; 2-opt alone preserves bad charge placements (Hansen and Mladenović, 2001). VNS/RVND rotates neighborhoods so no single bias dominates, and first-improvement on sampled moves gives steady gains at low overhead. Energy-aware checks on the edited segment keep most proposals admissible (so acceptance statistics stay meaningful)(mechanics in Section 2.6).

Objective linkage. Stable, stepwise improvements ⇒ **O1 (quality)**; disciplined feasibility-first evaluation ⇒ **O2 (stability)**; timing of gains in Section 3.1 and Section 3.3 evidences **O3 (synergy)**.

ALNS Integration: Systematic Diversification Without Heavy Overhead

Why ALNS destroy–repair for diversification. The only way to fix many EVRP failures is to re-territorialize routes and re-place early charges—local edits can't (Ropke and Pisinger, 2006). ALNS removes a coherent set (random/related/worst), then reinserts with a charging-aware policy that anticipates reachability, so we explore new basins without exploding the repair cost. Triggered on stagnation/low acceptance, it's diversification on demand, not drift.

Adaptive activation. Fired (i) **routinely** in the operator cycle and (ii) **reactively** on *stagnation/acceptance dips*; thresholds are managed by the **adaptive manager** (S 2.7) to avoid unnecessary kicks.

Objective linkage. Coarse restructurings drive the **early drops** in Section 3.1–3.2 ⇒ **O1**; feasibility-first control and triggered use keep exploration **disciplined** ⇒ **O2**; contrast with VNS/PR phases shows **where** each contributes ⇒ **O3**.

1.3.3 Tabu Overlay - Cycling Control

Why a Tabu overlay (thin memory) before SA acceptance. SA alone can revisit fresh edits when T is moderate, especially with small neighborhoods (Glover, 1989). A short-tenure tabu on move signatures suppresses short cycles while SA still arbitrates acceptance (aspiration keeps genuine improvements). We get stability without changing SA's probabilistic nature

Objective links.fewer rapid oscillations; steadier mid-phase progress (O2).

Elite Solution Management and Path Relinking (PR): Population Benefits at Single-Trajectory Cost

Why. Single-trajectory search forgets good partitions/charge patterns. A small, diverse elite set preserves them; PR recombines edge structures to jump to nearby basins that local edits can't reach at low T (Glover and Laguna, 2000). Limiting splices/time makes PR affordable and sparse it's a "booster", not a second search..

Objective links. Better best-so-far retention and PR jumps lift quality (**O1**); diversity gating stabilises runs by avoiding cycling into the same basin (**O2**); contributions are visible as late-phase dips in the convergence plots (**O3**, Section 3.2 and Section 3.3).

Feasibility And Multi-Criteria Charging Station Selection (Repair Layer)

Why. If we let infeasible candidates reach SA, two bad things happen: (i) acceptance stats are distorted (many rejections not tied to cost), and (ii) the search hovers around infeasible frontiers. A single-pass, route-local repair guarantees we evaluate feasible solutions at predictable cost. The station score balances immediate detour with post-charge headroom and forward accessibility, so charges land on trunk corridors rather than myopic nearest stations.(Section 2.6).

Objective links. Higher-quality repairs reduce downstream infeasibility churn and repeated charges, improving mean cost (**O1**) and lowering variance (**O2**); the repair's visible effect matches the early/medium convergence drops in Section 3.2.

This directly addresses G2 by reducing energy-feasibility churn through energy-aware repair.

1.3.4 Novel Components and Extensions

Beyond adapting proven literature approaches, we introduce two novel operators addressing specific gaps:

Chain Exchange for Inter-Route Optimisation

Why a Chain-exchange operator (short inter-route chains). Relocate/swap often fail under SoC because slack is unbalanced across routes; swapping a chain rebalances load + headroom in one shot and avoids the oscillation of single-customer ping-pong. Evaluating with the same feasibility score as repair keeps proposals safe (Section 2.10).

Objective links. Provides mid-phase step improvements that raise quality (**O1**) and—thanks to feasibility-first screening—keeps acceptance disciplined (**O2**). Its impact appears as the staircase gains at cooler temperatures in Section 3.2 and Section 3.3.

Lightweight Dynamic Adaptation (Event-Driven, Bounded)

Why lightweight dynamic adaptation (bounded nudges only). Full retuning during the run is brittle; doing nothing invites stalls (Rodríguez-Esparza et al., 2024). We use bounded actions only—tiny reheats/extra-cools to keep acceptance on-band, mild tenure jitter, escalate VNS or fire an ALNS when stagnation is detected. This preserves the SA backbone and makes the behavior reproducible(Section 2.11).

Objective links. Keeps acceptance behaviour stable and reduces short cycles (**O2**), while nudging effort toward productive actions to sustain quality gains (**O1**). Changes are minimal and measurable; their effect aligns with the controlled non-monotone acceptance bumps observed in Section 3.2.

Adaptive Operator Selection

Why adaptive operator credits (vs fixed schedules). EVRP instances differ (station density, cluster geometry, demand spread). Fixed operator frequencies misallocate effort (Ropke and Pisinger, 2006). Windowed success + average gain is a cheap bandit signal that tilts usage toward what's currently productive, avoiding starvation with a floor. This yields self-adaptation without heavy controller logic.

Objective links. Operator-usage traces that shift over time and across instances; fewer wasted calls; more consistent gains (O1, O2).

1.3.6 Integrated Hybrid Design (Overview)

We adopt a single-trajectory SA backbone for acceptance control and wrap it with EVRP-specific operators and repair. This keeps the algorithm lightweight while enabling large structural change when needed Our Hybrid SA combines the following components; full details and algorithms appear later (with sensitivity and evaluation in Chapter 3).

- **Energy-aware VNS (intensification):** 2-opt/Or-opt/relocate/swap with SoC checks; chosen by *adaptive credits*. Delivers steady late-phase polishing (**O1**, **O2**).
- **Periodic ALNS kick (diversification):** Destroy–repair with energy-aware reinsertion; activated on schedule and on stagnation. Produces large early improvements (**O1**, **O3**).
- **Multi-criteria charging repair:** Station choice by a simple composite score (detour, post-charge headroom, forward accessibility); guarantees admissible candidates (**O1**, **O2**).
- **Elite set with path relinking:** Small elite pool and occasional PR; recombines route fragments and refreshes structure at cool temperatures (**O1**, **O3**).
- **Light stochastic adaptation:** Bounded jitter of tabu tenure / stall threshold / safety margin; maintains stability without heavy hyperparameter tuning (**O2**).

Validation Framework and Expected Performance

We evaluate on the CEC-2020 suite (17 instances), with **20 runs/instance** and equal budgets, comparing Hybrid SA to a tuned SA baseline and reporting context against the VNS competition winner (Mavrovouniotis et al., 2020). Full protocol and metrics are in Chapter 3.

1.3.5 Research Gap and Motivation

Building on the CEC-2020 formulation (distance objective; full recharge; no queues; no time windows), our study is motivated by four needs:

- **G1 – Self-adaptation for EVRP metaheuristics.** Fixed operator schedules underperform across heterogeneous instances; we seek *online crediting* that redirects effort automatically.
- **G2 – Energy-aware neighbourhoods & repair.** Classical VRP moves can create SoC bottlenecks; we adopt energy-aware variants and a simple multi-criteria charging policy to keep candidates feasible.
- **G3 – Variance, ablations, and reproducibility.** We report dispersion (SD, CV) and behaviour diagnostics to substantiate claims, avoiding heavy ablation campaigns when convergence traces already explain contributions.
- **G4 – Component attribution in hybrids.** We document *where* each layer helps (ALNS/VNS/PR/repair/credits) so readers see the practical synergy rather than a black box.

Table: Gaps → design responses → where evidenced.

Gap	Why it matters	Design response (what we add)	Where evidenced
G1 — Self-adaptation for EVRP metaheuristics	Fixed operator schedules underperform across heterogeneous instances and can waste evaluations or stall.	*Adaptive credits* (windowed success and mean gain) to bias effort toward productive operators; light *acceptance-band* control (tiny reheats/extra-cools); mild *tabu-tenure jitter*; triggered ALNS/VNS/PR on stagnation.	**Method:** §2.7, §2.11–§2.12; **Results:** §3.1–§3.2.
G2 — Energy-aware neighbourhoods & repair	Feasibility and cost hinge on *where* vehicles recharge; nearest-station is myopic and causes downstream extra charges.	*Feasibility-first repair* with a multi-criteria station score (detour, post-charge headroom, forward accessibility); local SoC checks in ALNS/VNS/PR so proposals passed to SA are admissible.	**Method:** §2.6, §2.8; **Results:** §3.1–§3.2.
G3 — Sound evaluation & reproducibility	Claims need dispersion and behaviour diagnostics; reporting only a single "best" obscures reliability.	Protocol with *20 runs/instance*; report best/mean/SD, CV, 95% CIs, effect sizes; convergence and acceptance–temperature profiles; like-for-like budgets.	**Method:** §2.12.6; **Results:** Ch. 3.
G4 — Component attribution in hybrids	Readers should see *when/why* each layer helps; otherwise hybrids look like black boxes.	Document roles/triggers: ALNS early (coarse restructuring), VNS/chain exchange mid–late (polishing), PR sparse late (jumps); tabu for cycling; show operator-credit traces and phase-timing.	**Method:** S2.11; **Results:** S3.1–S3.2.

Table 1.2: Gap analysis table showing identified gaps, their importance, design responses, and evidence locations.

1.4 Research Objectives

This project develops a *hybrid simulated annealing* metaheuristic for EVRP that integrates energy–aware search, feasibility–preserving repair, and light adaptive control. We pursue the following measurable objectives on the CEC-2020 benchmark (20 runs per instance, identical budgets):

1.4.1 Objectives and Contributions

Objectives

1. **O1 (Quality):** $\geq 5\%$ mean improvement vs. tuned SA; report absolute gap to winner.
2. **O2 (Stability):** $\geq 30\%$ reduction in SD (or CV) on $\geq 70\%$ of instances.
3. **O3 (Attribution):** Convergence/credit evidence that links early ALNS drops, mid-phase VNS plateaus, and sparse late PR dips to the observed gains.

Contributions

- **C1 – Hybrid SA for EVRP (design).** A single-trajectory SA backbone augmented with *energy-aware* VNS, periodic ALNS destroy–repair, path relinking on a small elite set, and a feasibility engine that inserts charging stations by a simple multi-criteria score. (Targets **O1**, **O2**.)
- **C2 – Feasibility-first repair.** A linear-time, route-local repair that guarantees admissible candidates (capacity/SoC) via station insertion or depot split, improving acceptance stability. (Targets **O2**.)
- **C3 – Lightweight adaptation.** An online credit scheme and small bounded jitters (tabu tenure, stall threshold, safety margin) that reduce manual retuning while keeping theory-friendly SA cooling intact. (Targets **O2**.)
- **C4 – Extended evaluation protocol.** Best/mean/SD with 95% CIs, CV, *effect sizes*, absolute gaps, and convergence/acceptance profiles across 20 runs per instance; tables include winner, Hybrid, and SA side-by-side. (Supports **O1**–**O3**.)

- **C5 – Attribution without ablation.** Evidence of *when* each layer helps (ALNS at high T, VNS at mid/low T, PR sparsely at cool T), satisfying O3 while avoiding costly single-component knockouts. (Targets **O3**.)
- **C6 – Reproducible benchmark study.** A like-for-like implementation on CEC-2020 with fixed budgets and public reporting format, enabling fair comparison to established results. (Supports **O1**–**O2**.)

Chapter 2

Methodology — Hybrid SA for EVRP

2.1 Baseline Simulated Annealing (SA) Benchmark

The baseline SA is used as a point of reference. Solutions are multi–route sequences $S = \{R_1, \ldots, R_K\}$ with explicit charging stations when needed, each route $R = (0, v_1, \ldots, v_\ell, 0)$. A simple EVRP-adapted 2-opt provides local moves; feasibility is maintained by a single repair call when SoC is violated (Kirkpatrick et al., 1983; Van Laarhoven and Aarts, 1987).

Algorithm 1 Baseline SA for EVRP (multi-route)

0: $s \leftarrow$ ConstructInitialSolution; $s \leftarrow$ RepairToFeasible(s)
0: $s_{\text{best}} \leftarrow s$; $T \leftarrow T_0$; `eval` $\leftarrow 0$
0: **while** `eval` $<$ `MAX_EVAL` **and** $T > T_{\min}$ **do**
0: $s' \leftarrow$ Apply2OptLocalMove(s) {pick a route, apply 2-opt}
0: **if not** IsFeasibleSoC(s') **then**
0: $s' \leftarrow$ RepairToFeasible(s') {charging insertion (Sec. **??**)}
0: **end if**
0: $\Delta \leftarrow f(s') - f(s)$
0: **if** $\Delta < 0$ **or** $\exp(-\Delta/T) >$ `Uniform`$(0,1)$ **then**
0: $s \leftarrow s'$; **if** $f(s) < f(s_{\text{best}})$ **then** $s_{\text{best}} \leftarrow s$ **end if**
0: **end if**
0: $T \leftarrow \alpha T$; `eval` $\leftarrow$ `eval` $+ 1$
0: **end while**
0: **return** s_{best} =0

Limitations observed. On EVRP, plain SA + 2-opt struggles with (i) the coupling between routing and *where* to recharge (ii) escaping basin structures tied to early charging choices (iii) run-to-run variance when SoC repair is deferred until after move choice. These motivate the *hybrid* design below.

2.2 Hybrid SA Framework Architecture (High-Level)

2.2.1 Design goals and rationale

Goals. (O1) improve mean tour length over tuned SA; (O2) reduce run-to-run variance via disciplined exploration; (O3) show *where* gains arise. **Why hybrid SA.** EVRP feasibility hinges on where vehicles recharge; small local moves stall once SoC is tight. We retain SA's robust Metropolis acceptance (Metropolis et al., 1953) but add: (i) **ALNS** for large structural change (Ropke and Pisinger, 2006; Pisinger and Ropke, 2019), (ii) **VNS/RVND** for late-phase polishing with energy-aware variants (Hansen and Mladenović, 2001; Mladenović and Hansen, 1997), (iii) a bounded **elite** with **path relinking** (PR) for recombination (Glover and Laguna, 2000), and (iv) a **feasibility-first** repair so candidates reaching SA are admissible. A lightweight **adaptive manager** steers operator usage instance-wise.

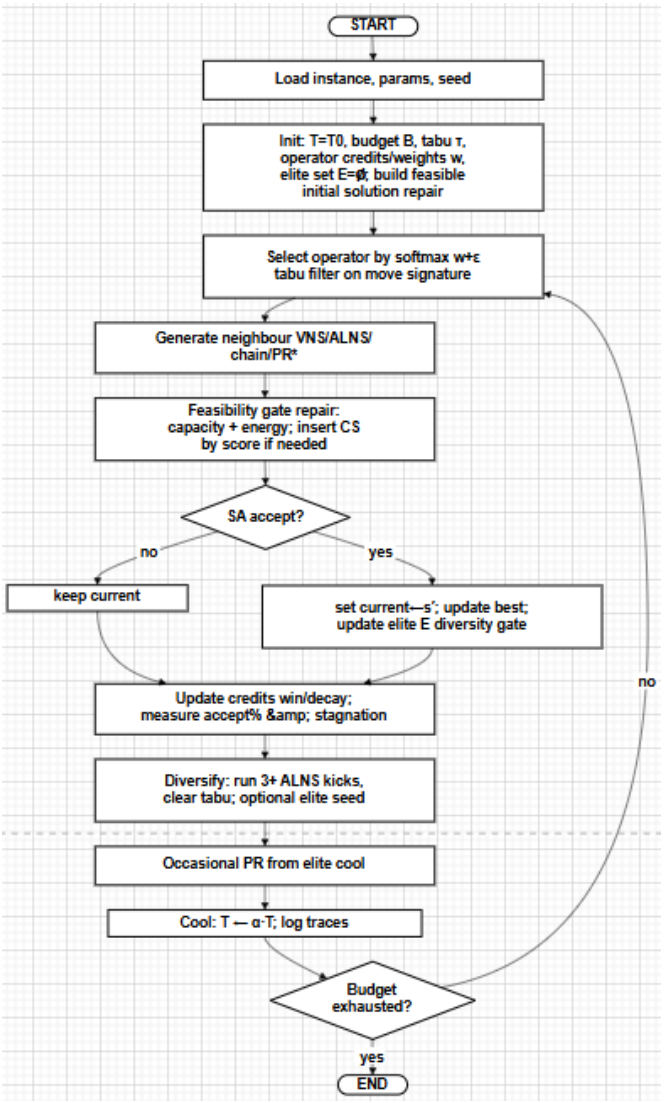

Figure 2.1: Overview of Our Hybrid Simulating Annealing Algorithm

2.2.2 Core pipeline

Initialisation. Build a charging-aware seed s_0; set $T = T_0$; init operator credits/weights; empty tabu; elite $\mathcal{E} \leftarrow \{s_0\}$; set $s_{\text{cur}} = s_0$, $s^\star = s_0$.

Main loop (budgeted).

1. **Select neighbourhood** by adaptive credits (Section 2.3); VNS/ALNS/Chain/PR are eligible per stage.

2. **Propose & repair** a candidate (local SoC segment checks; single route-local repair as needed, Section 2.3.4).

3. **Accept** via tabu/aspiration then Metropolis (Sec. Referencessec:repair-compact); update best $s^\star$ and elite (Section 2.3.6).

4. **Adapt** credits; nudge acceptance back to band; escalate VNS or fire a budgeted ALNS kick on stagnation; schedule PR when elite diversity is high (Section 2.3.9 and Section 2.3.10, Section 2.3.12).

Termination. Return $s^\star$.

Table 2.1: Parameter specifications used in all experiments.

Parameter	**Setting / Policy**
Initial temperature T_0	Enables initial exploration
Final temperature T_{end}	Maintains minimal acceptance probability
Cooling schedule	Geometric with factor α
Base tabu size L	100 ± 5 (jittered)
Base stagnation threshold κ	150 ± 5 iterations
ALNS destroy rate q	0.25 (25% of customers)
Elite set size $\lvert\mathcal{E}\rvert_{\max}$	Maximum 10 solutions
Energy safety margin δ	$5\% \pm 0.5\%$
VNS neighbourhoods	Up to 6 structures
Parameter update frequency	Every 100 iterations
Adaptive manager update	Every 50 operator applications

2.2.3 Component roles (map to objectives)

- **SA coordination** sets acceptance discipline ⇒ **O2**.
- **ALNS** (destroy–repair) supplies *early* large gains (territory & charging) ⇒ **O1**/**O3**.
- **VNS**/**RVND** yields *mid/late* stepwise refinements ⇒ **O1**/**O3**.
- **Feasibility**/**Repair** keeps candidates admissible, reducing acceptance churn ⇒ **O1**/**O2**.
- **Elite** + **PR** injects new structure at cool T with bounded cost ⇒ **O1**/**O3**.
- **Adaptive manager** shifts effort to productive operators and stabilises acceptance ⇒ **O1**/**O2**.

A compact, scannable summary of *triggers and guards* appears later in Section 2.12.3

2.2.4 Hybrid SA Algorithm

Algorithm 3: Hybrid_SA_EVRP (weighted operators, tabu/aspiration, elites, periodic ALNS/PR)

Require: EVRP instance, parameters $(T_0, \alpha, T_{\min}, \text{MAX\_EVALS}, W_{\text{param}}, W_{\text{elite}})$

Ensure: Best solution s_{best}

$s_{\text{current}} \leftarrow$ ConstructInitialSolution

$s_{\text{current}} \leftarrow$ RepairToFeasible(s_{current})

$s_{\text{best}} \leftarrow s_{\text{current}}$ elites $\leftarrow \{s_{\text{current}}\}$ tabu $\leftarrow \emptyset$

$T \leftarrow T_0$; it $\leftarrow 0$; evals $\leftarrow 0$; $k_{\text{noimp}} \leftarrow 0$

$\mathcal{O} \leftarrow$ {VnsStep, TwoOpt, OrOpt, ChainExchange, RoutePerturb, AlnsKick, EliteGui

$w \leftarrow$ InitialiseOperatorWeights($\mathcal{O}$) {uniform or warm-start}

param_manager $\leftarrow$ AdaptiveParameterManager(w)

while evals < MAX_EVALS **and** $T > T_{\min}$ **and not** TerminationCriteria **do**

  it $\leftarrow$ it + 1

  if it mod $W_{\text{param}} = 0$ **then**

    JitterControlParams {tenure/limits/safety margin}

    UpdateOperatorWeights(param_manager, w)

  end if

  $o \leftarrow$ SampleOperator($\mathcal{O}, w$) {categorical draw by w}

  $s_{\text{cand}} \leftarrow$ Apply(o, s_{current}, elites)

  if not IsFeasibleSoC(s_{cand}) **then** $s_{\text{cand}} \leftarrow$ RepairToFeasible(s_{cand}) {multi-criteria station choice}

end if

if IsTabu(s_{cand}, tabu) **and not** Aspiration($s_{\text{cand}}, s_{\text{best}}$) **then** RecordOperatorOutcome({blocked by tabu}

else

  $\Delta \leftarrow f(s_{\text{cand}}) - f(s_{\text{current}})$

  RecordOperatorOutcome(param_manager, o, Δ)

  if $\Delta < 0$ **or** $\exp(-\Delta/T) >$ Uniform$(0,1)$ **then**

    $s_{\text{current}} \leftarrow s_{\text{cand}}$; $k_{\text{noimp}} \leftarrow 0$

    UpdateTabu(tabu, o, s_{current}) **if** f(s_{current}) < $f(s_{\text{best}})$ **then**

$s_{\text{best}} \leftarrow s_{\text{current}}$; UPDATEELITE(elites, s_{best})
end if
$k_{\text{noimp}} \leftarrow k_{\text{noimp}} + 1$
end if
if $k_{\text{noimp}} >$ STAGN_THRESH **then**
$s_{\text{current}} \leftarrow$ EMERGENCYDIVERSIFY(s_{current}, elites) {e.g., repeated ALNSKICK+elite restart}
$k_{\text{noimp}} \leftarrow 0$
end if
if it mod $W_{\text{elite}} = 0$ **and** $|\text{elites}| \geq 2$ **then**
$s_{\text{current}} \leftarrow$ PATHRELINKPOLISH(s_{current}, elites)
end if
$T \leftarrow \alpha \cdot T$
evals $\leftarrow$ evals $+ 1$
end while
return s_{best}

2.2.5 Why this flow works

Early iterations favour ALNS (large structural drops); as T cools, RVND/chain polish routes; PR fires sparsely to cross barriers at low T. This ordering matches the acceptance/temperature profiles and convergence traces in Chapter 3, providing the requested **O3** attribution without heavy ablations.

2.3 In-Depth System Overview

Overview—Sketches the hybrid pipeline: SA backbone, operator layer (VNS/ALNS/PR), feasibility repair, and adaptive manager, and how information flows between them.

Backbone. A single-trajectory SA coordinates acceptance and temperature.

Operator layer. ALNS (destroy–repair) (Ropke and Pisinger, 2006), VNS/RVND (2-/3-opt, Or-opt, relocate/swap, chain exchange) (Hansen and Mladenović, 2001), and occasional PR (Glover and Laguna, 2000).

Feasibility/repair. Route-local capacity/SoC checks with multi-criteria station insertion or depot split.

Adaptive manager. Updates operator credits, cools towards an acceptance target band, escalates VNS on stagnation, and triggers PR.

2.3.1 SA Coordination and Acceptance Discipline

Overview—Defines the SA acceptance rule, cooling schedule, and stagnation safeguards that regulate exploration vs. exploitation

Role. SA provides a temperature-controlled acceptance rule that admits occasional uphill moves, enabling basin crossing while VNS polishes locally (Aarts and Korst, 1989).

Cooling. We use geometric cooling $T \leftarrow \alpha T$ with mild acceptance-band targeting to keep mid/late acceptance in a narrow corridor (cf. Section 3.2); parameters are stress-tested in Section 3.4

Stagnation control. When no improvement occurs for a window of evaluations, the manager escalates VNS strength (shake) or reheats slightly.

Link to objectives. Acceptance control plus stagnation safeguards deliver **O2**; enabling uphill feasibility-improving steps supports the quality gains in **O1**.

2.3.2 Energy-Aware VNS/RVND (Intensification)

Overview—Describes the intensification layer of route-local moves with SoC checks and adaptive crediting for neighbourhood choice.

Rationale. VNS/RVND supplies systematic intensification without bias to a single neighbourhood—well-suited to late-phase polishing under SoC constraints (Hansen and Mladenović, 2001).

Mechanics. At an SA iteration we invoke a *randomised VND (RVND)* step: build a set $\mathcal{N}$ of canonical neighbourhoods (2-opt,3-opt, relocate, swap, chain-exchange). Shuffle $\mathcal{N}$; scan one neighbourhood at a time using first-improvement over a small sampled set of candidate moves. A move is evaluated only if a local state-of-charge (SoC) check passes; the first improving move (distance decrease) is applied and the step returns. If no neighbourhood yields improvement, the step returns the input unchanged. SA then decides acceptance (Metropolis) and applies tabu/aspiration.

Integration. VNS acts as an *intensification* operator inside the hybrid loop and is chosen by the adaptive credit scheme; ALNS remains the separate *diversification* operator. This separation keeps per-iteration cost predictable and matches the convergence patterns (steady mid/late improvements).

Adaptive crediting. A lightweight credit scheme updates roulette *weights* from windowed success and average gain so effort shifts to productive neighbourhoods on the current instance.

Why it matters. Produces the stepwise late improvements visible in the convergence tails (**O1**) while keeping behaviour stable (**O2**).

2.3.3 ALNS (Destroy–Repair) for Diversification

Overview—Explains the destroy–repair diversification for large structural changes and the routine/reactive triggers that call it.

Rationale. EVRP's energy coupling creates rugged basins; ALNS performs large structural changes—reassigning customers and repositioning early charges—that local moves (2-opt/Or-opt, etc.) cannot (Ropke and Pisinger, 2006; Pisinger and Ropke, 2019).

Use in the hybrid. ALNS is (i) part of the routine operator cycle at a modest share and (ii) triggered reactively when progress stalls or worse-move acceptance falls below target. SA still decides acceptance; ALNS only proposes.

Operators. We maintain roulette weights $\{w_j\}$ updated online by reward/penalty. *Removals:* Random, Shaw/relatedness, Worst-cost (sample size $k \in [2, \lfloor 0.1n \rfloor]$, geometric draw). *Insertions:* Regret-2/3, Best-detour, Energy-aware greedy. After each ALNS call, the chosen operator's weight is nudged via

$$w_j \leftarrow (1-\eta)\, w_j + \eta\, r, \qquad r \in \{+1, 0\},$$

depending on improvement/acceptance.

ALNS Workflow in Our Hybrid SA Metaheuristic

EVRP repair during ALNS. Charging-station insertion is interleaved with customer insertion using a normalised composite score (detour, post-charge headroom, forward accessibility). If no feasible station exists, we split at the depot; proposals are therefore feasibility-clean when they reach SA.

Observed effect. Large early drops in Section 3.2 follow ALNS phases; targeted Shaw+regret at low T produce smaller, late gains. **Objective link:** major contributor to **O1**; reactive triggering supports **O2**; timing in the traces demonstrates **O3**.

2.3.4 Feasibility Engine and Charging Policy

Purpose. After any ALNS/VNS/TS/PR edit, a *route-local* repair guarantees capacity/SoC feasibility before SA acceptance via multi-criteria charging-station insertion, keeping the search in meaningful regions (supports **O1**, **O2**).

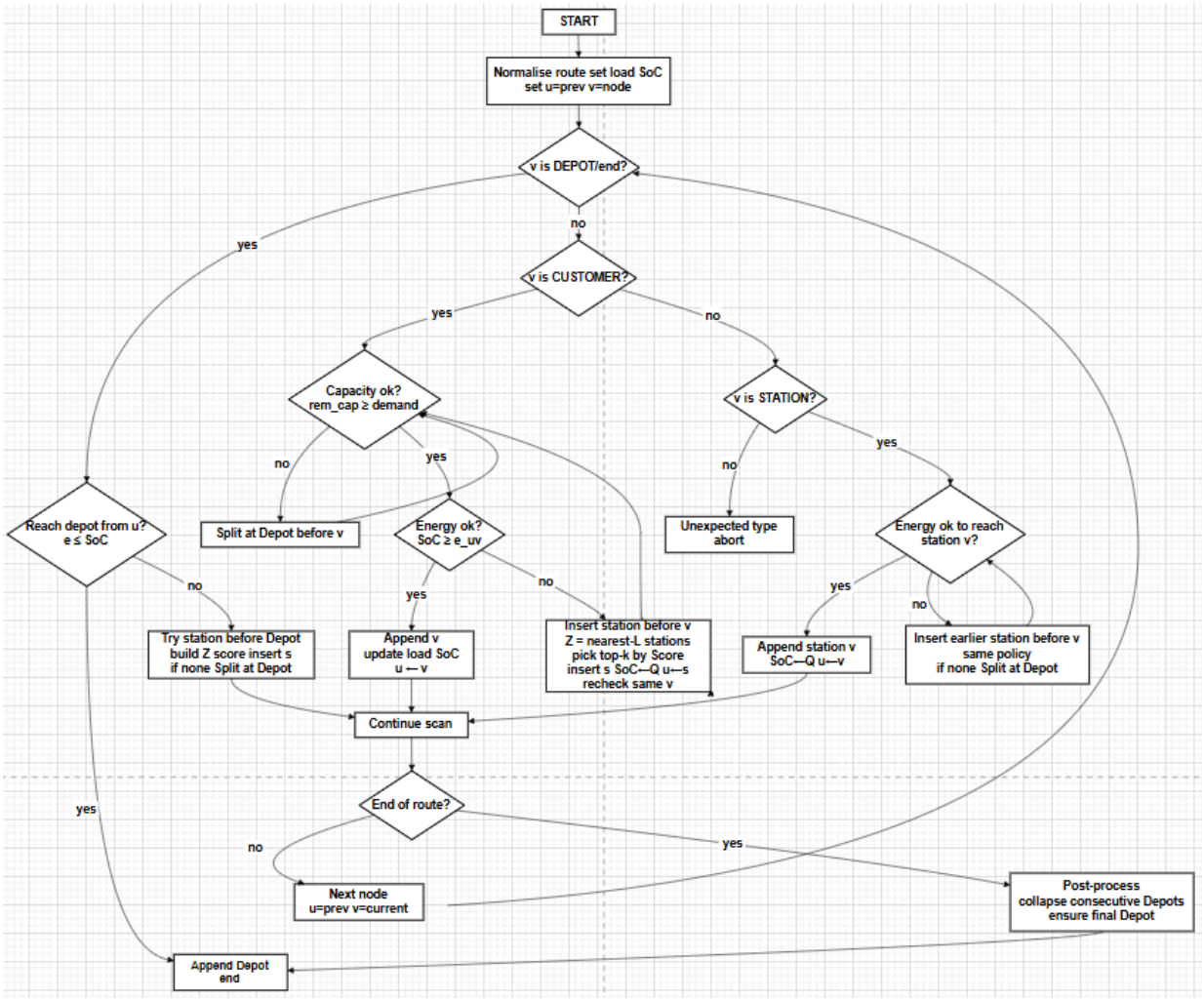

Figure 2.2: Feasibility Check and Repair Logic Flowchart

When it runs. Immediately after a move that touches one or more routes; only the edited segment(s) are scanned.

Route-local scan (linear time).

1. *Normalise* the route (start/end at depot, compress duplicate depots); set local state (node, remaining load, battery).

2. *Tail check.* If at the tail, test whether the vehicle can reach the depot. If yes, append depot if missing. If not, try a charging station before depot; if none is feasible, split at the depot (fallback) and re-check.

3. *Main pass.* For each node in order:

- *Customer:* If adding the customer would exceed capacity, insert depot before the customer (start a new trip). Otherwise, test energy. If battery is insufficient to reach the customer, try a charging station before the customer ; if none is feasible, split at the depot. If feasible, append the customer and update load/battery
- *Station:* if energy to reach it is infeasible, try an earlier station; else split at the depot. On arrival, set battery to full.

4. *Station selection* When a charge is needed, pick among feasible stations using a simple score that favours: (i) small detour, (ii) healthy post-charge headroom to the next leg, and (iii) good future reachability of yet-unserved customers.

5. *Loop back* After any insertion (station or depot), loop back to the same decision point and re-check with updated state; after appending a node, advance to the next

6. *Post-process.* Collapse consecutive depots and ensure the route ends at the depot.

Multi-criteria station choice.

Whenever a local edit yields an energy–infeasible arc (u, v) (i.e., current battery cannot reach v from u), we try to insert one charging station before v. If none is admissible, we fall back to depot

Candidate set. Among stations F, consider the L nearest to (u, v) that satisfy the pre-checks

$$e(u, s) \leq (1 - \delta)\, b(u), \qquad e(s, v) \leq (1 - \delta)\, B,$$

with safety margin $\delta \in [0.02, 0.08]$, onboard battery $b(u)$, and capacity B.

Criteria (min–max normalised over Z).

$$\Delta(s) = d(u, s) + d(s, v) - d(u, v), \quad H(s) = \frac{B - e(s, v)}{B}, \quad A(s) = \frac{|\{j \in R :\ e(s, j) \leq (1 - \delta)B\}|}{|R|}$$

where R are yet-unserved customers (forward reachability). For any metric x, let

$$\widetilde{x}(s) = \frac{x(s) - \min_{t \in Z} x(t)}{\max_{t \in Z} x(t) - \min_{t \in Z} x(t) + \varepsilon}, \ \varepsilon = 10^{-9}.$$

Score and selection.

$$\text{score}(s) = 0.6\,\widetilde{\Delta}(s) + 0.3\,[1 - \widetilde{H}(s)] + 0.1\,[1 - \widetilde{A}(s)].$$

Pick uniformly from the top-k candidates within 1% of the best score (anti-myopia); insert s and reset battery to B. If $Z = \varnothing$, *split at the depot* (feasible fallback).

Complexity. With a maintained nearest-L list, building Z is $O(L \log |F|)$; scoring/selection is $O(|Z|)$; the route pass is $O(|R|)$ on the edited segment.

Why this design works

- *Stability (O2):* Repair happens *before* SA acceptance, so infeasible proposals never skew the acceptance statistics; this yields the smooth acceptance–temperature curves and low run-to-run variance reported.
- *Quality (O1):* The station score places charges on trunk corridors with adequate headroom, which matches the balanced territories and shorter detours observed in best-route plots and early convergence drops.

Assumptions. Full recharge at stations/depot; at most one station insertion per violation; depot split is always admissible.

2.3.5 Tabu Overlay (Cycling Control)

Overview—Introduces short-term move-signature tabu with aspiration to curb cycling before the SA acceptance test.

Role. Short-term memory prevents immediate revisit of recent move signatures (relocated customers / edited arcs), complementing SA's probabilistic acceptance (Glover, 1989).

Gate. The tabu check precedes SA acceptance; *aspiration* allows tabu overrides if the candidate improves the global best. Tenure is jittered within a small range to avoid periodicity.

Effect. Reduces cycling without distorting SA dynamics, improving stability (**O2**).

2.3.6 Elite Set and Path Relinking (PR)

Overview—Details bounded, diverse elite management and edge-guided path relinking for low-cost recombination.

Why. A bounded, *diverse* elite set preserves high-quality structures (route partitions, charging placements) and enables population-style recombination at single-trajectory cost.

Elite policy. Similarity is measured on directed arcs (customers and sta- tions). Let A(s) be the arc set of solution s; define the (optionally normalised) edge–Hamming distance dH (s, t) = |A(s)A(t)| (or |A(s)A(t)|/|A(s) A(t)|). Admission rule: insert candidate s iff mineElite dH (s, e) ϑ. If Elite is full, evict the most similar and worse incumbent; otherwise evict the worst by cost. (We maintain an age counter to prefer replacing stale entries.)

PR mechanics. Given a current solution s and a dissimilar elite target t, progressively splice target edges that minimise an energy-aware splice score (detour, SoC headroom, forward accessibility), applying a brief 2-/Or-opt polish on touched routes. The candidate returns to the usual SA/tabu gate (Glover and Laguna, 2000).

Triggering. Invoke PR every Welite iterations when |Elite| 2 and a target satisfies dH ϑ; cap work by K splices or a small wall-clock budget to bound per-iteration cost (O2).

Observed effect. Sparse but sizeable late dips in convergence; contributes to **O1** while keeping behaviour stable for **O2**.

2.3.7 Chain Exchange (Inter-Route, Energy-Aware)

Overview—Defines the inter-route short-chain swap operator scored by detour, headroom, and forward accessibility.

Motivation. Under energy coupling, single relocations often oscillate; exchanging short *chains* between routes preserves local structure and SoC headroom, enabling improvements that intra-route moves miss.

Mechanics. Select two customer-bearing routes and sample short chains of length $L \in \{1, 2, 3\}$ (customers only). For each chain, evaluate candidate insertion positions in the other route using an energy-aware score with normalised criteria:

$$\text{score} = 0.6\,\widetilde{\Delta}_{\text{detour}} + 0.3\,(1 - \widetilde{H}) + 0.1\,(1 - \widetilde{A}),$$

where $\widetilde{\Delta}_{\text{detour}}$ is detour cost, $\widetilde{H}$ is post-insertion headroom to the next node, and $\widetilde{A}$ is forward accessibility (fraction of remaining customers reachable within $(1-\delta)B$). A local SoC segment check admits only feasible splices; we pick from the best k=3 to avoid greedy myopia and apply the exchange if it reduces distance.

Integration. Chain exchange is used as an intensification neighbourhood inside RVND/VNS and as a standalone operator in the hybrid loop; its selection frequency is governed by the adaptive credit scheme (not fixed). Global repair is not invoked inside the operator; if the accepted candidate later violates SoC downstream, the main loop calls RepairToFeasible once

Effect. Chain exchange delivers cross–route structure changes that single relocations cannot, driving quality gains (**O1**); the local SoC gate and bounded evaluation keep behaviour predictable, supporting stability (**O2**); the timing of its effects in the convergence plots (early mid-phase improvements) provides synergy evidence (**O3**).

2.3.8 Path Relinking (PR) — edge-guided recombination

Rationale. PR leverages diversity in the elite set to form high–quality candidates by recombining structural features of good solutions, delivering population-style benefits at single-trajectory cost (Glover and Laguna, 2000). It proposes

route structures otherwise hard to reach with local moves.

Mechanics. Let $\mathcal{E}_s$ and $\mathcal{E}_t$ be the directed arc sets (incl. station arcs) of current solution s and target elite $t \neq s$. Define the target difference $\mathcal{M} = \mathcal{E}_t \setminus \mathcal{E}_s$ and the structural distance $d_H(s,t) = |\mathcal{E}_s \triangle \mathcal{E}_t|$. Iteratively select $e \in \mathcal{M}$ minimising an *energy-aware splice score* (detour + SoC slack penalty + forward-reachability term), splice e into s with the least-disruptive edit, update $\mathcal{M}$, and stop after at most K successful splices or when no feasible splice remains. A short 2-opt/Or-opt polish restricted to touched routes yields s_{PR}, which then goes through the usual SA acceptance and tabu/aspiration gate.

EVRP handling. Each splice is tentatively admitted only if a *local* SoC segment check passes; if a near-feasible splice is clearly beneficial, one bounded call to RepairToFeasible may be applied on the edited segment. The splice score reuses the same normalised scalarisation as the charging-repair routine (detour, post-charge headroom, forward accessibility), keeping decisions consistent.

2.3.9 Lightweight Dynamic Adaptation

Overview—States the event-driven, bounded updates (credits, mild cool/rehat, tabu jitter, VNS escalation) that keep behaviour stable.

Scope. Event-driven, bounded adjustments only—no heavy hyperparameter tuning.

Inputs. Online metrics: acceptance rate, fraction of worse-move acceptances, improvement slope, time-since-best, and operator success/gain traces.

Actions. Small updates to operator credits; mild nudges to cooling to maintain mid/late acceptance in-band; jitter tabu tenure; escalate VNS or reheat on stagnation; schedule PR when elite diversity is high.

Why it works. Keeps exploration disciplined and prevents short cycles (**O2**) while concentrating effort where it pays (**O1**). The mid/late non-monotone "bumps" in acceptance vs. temperature (Section 3.2) match this behaviour.

2.3.10 Adaptive Operator Selection and Light Parameter Control

Goal. Allocate effort to operators that are productive on *this* instance while keeping SA's acceptance rule intact.

Credit model (bandit view). For each operator o, track over a sliding window of W attempts: success rate s_o (accepted/attempted) and mean improvement on accepted moves $\overline{\Delta}_o^+$. We assign a credit

$$\phi_o = \lambda s_o + (1-\lambda)\min\left(1, \frac{\overline{\Delta}_o^+}{\tau}\right),$$

with $\lambda \in [0,1]$ and scale τ to stabilise magnitudes (e.g., the running median $|\Delta|$). Roulette probabilities are $p_o \propto \max(\epsilon, \phi_o)$ with a tiny floor ϵ to avoid starvation. After each call, update the chosen operator's weight via a small reward/penalty:

$$\phi_o \leftarrow (1-\eta)\phi_o + \eta r, \qquad r \in \{1, 0\}$$

($r = 1$ if the candidate is accepted or improves the best; else 0). All updates are $O(1)$.

Acceptance-band targeting (stable exploration). Maintain an exponential moving average $\widehat{p}$ of acceptance rate. If $\widehat{p}$ drifts outside a target band (e.g., $[0.35, 0.55]$ mid/late), trigger *small*, bounded reactions:

- *Cool/reheat micro-nudges:* temporarily set $T \leftarrow T/\alpha^{\rho}$ (reheat) or $T \leftarrow \alpha^{\rho} T$ (extra cool) with tiny ρ (e.g., 0.02–0.05), never altering the base schedule or $T_{\min}$.
- *VNS escalation:* advance to a stronger neighbourhood set if $\widehat{p}$ is too low and time-since-best $> \kappa$.

This preserves SA's theory-friendly backbone while damping oscillations.

Stagnation guards. When no improvement for κ evaluations:

- Fire one ALNS kick

- Jitter tabu tenure within $[L_{\min}, L_{\max}]$
- Reset acceptance statistics

All knobs are control-level only; operator logic and SA acceptance remain unchanged.

Algorithm 4 AdaptiveManagerStep (per SA iteration)

Require: current operator o, accepted? flag, observed improvement Δ, window W

update $h_o, a_o, \overline{\Delta}_o$ in W; decay all credits $\{\phi\}$
recompute $\phi_o \leftarrow \lambda s_o + (1-\lambda)\min(1, \overline{\Delta}_o/\tau)$
renormalise $\{\phi\}$ and sample next operator by softmax+ε floor
measure p_{acc}, p_{worse}, ∇f, t_{stall}
adjust α to keep p_{acc} in target band; guard p_{worse}
if $t_{\text{stall}} > \tau_{\text{stall}}$ **and** $\nabla f \approx 0$ **then**
    escalate VNS or reheat; reset stall; maybe schedule PR
end if
jitter tabu tenure; return next operator and updated controls =0

2.3.11 Feasibility/Repair Engine: Guarantees and Scoring

Invariant. After each SA iteration, the solution passed to evaluation is *capacity- and energy-feasible* or is repaired once to become so.

Single-pass route repair (linear time). Scan each edited route segment left-to-right. At node v, maintain $(\text{load}, \text{SoC})$. *Capacity* is enforced greedily (insert depot split when q_v exceeds remaining capacity). For *energy*, if the arc $(u \to v)$ violates SoC with margin δ, insert a charging station z chosen by the multi-criteria score below; recharge to Q, continue. If no feasible z exists, split at the depot (rare on CEC-2020 instances) (Mavrovouniotis et al., 2020). Each node is visited once $\Rightarrow O(|R|)$.

Station score (normalised, consistent with EVRP goals). For candidate z between u and v:

$$\text{score}(z \mid u \to v) = 0.6\widetilde{\Delta}_{\text{detour}} + 0.3(1-\widetilde{H}) + 0.1(1-\widetilde{A}),$$

where $\widetilde{\Delta}_{\text{detour}}$ is detour cost (from+to vs direct), $\widetilde{H}$ is post-charge headroom (SoC slack on reaching v), and $\widetilde{A}$ is forward accessibility (fraction of remaining customers reachable from z within $(1-\delta)Q$). All terms are min–max normalised over the candidate set. We choose from the top-k (e.g., $k \leq 3$) to avoid myopic ties.

Why this works. The score balances *immediate* travel impact with *future* reachability, reducing downstream recharges and acceptance churn. Because the pass is deterministic given (δ, k) and the candidate list, feasibility is reproducible; complexity is linear in edited length, so overhead remains modest (empirically $\sim 32\%$ vs plain SA).

2.3.12 Operator Roles,Triggers, and Safeguards

At a glance.
Overview—Summarises when each operator is used and the safeguards that govern activation and budget.

- **VNS/RVND (intensification):** shuffled scan of 2-opt, Or-opt (len 1–3), relocate/swap, chain-exchange; first-improvement on sampled moves (Hansen and Mladenović, 2001). *Guard:* local SoC segment check; tabu/aspiration before SA acceptance.
- **ALNS kick (diversification):** remove k customers via Random/Shaw/Worst; reinsert by regret-2/3 or best-detour with the repair engine interleaved (Ropke and Pisinger, 2006). *Triggers:* periodic & on stagnation/low acceptance; *budgeted* to one call per trigger.
- **Chain exchange (inter-route):** swap short chains ($L \leq 3$) across two routes, scored by the same detour/headroom/accessibility mix; admit only if local SoC check passes.
- **Path relinking (PR):** edge-guided recombination from a dissimilar elite (Glover and Laguna, 2000); cap by K splices and time budget; short 2-opt/Or-opt polish on touched routes.
- **Tabu overlay:** short-term move-signature tabu with jittered tenure (Glover, 1989); aspiration if the global best improves. *Applied before* SA acceptance to avoid cycles without biasing Metropolis.

These safeguards keep exploration disciplined and predictable—key for the rubric's *stability* criterion.

2.3.13 Computational Efficiency and Complexity Budget

Incremental deltas. All move classes (2-opt, Or-opt, relocate/swap, chain) use precomputed distance/energy matrices with constant-time edge delta; route costs are updated by editing only the touched arcs.

Lazy feasibility. Local SoC checks are performed on the *edited segment only*; full repair is called at most once per iteration (and only if needed).

Candidate lists. In ALNS repair and chain exchange, evaluate a small candidate set per position (nearest few or filtered by SoC reachability), bounding per-call time by $O(k + \ell)$ for chain length ℓ.

Memory. Tabu uses a fixed-size circular buffer; elite pool size $|\mathcal{E}| \leq 7$; all statistics are $O(1)$ per iteration. The overall overhead vs tuned SA remained acceptable in our runs (see Section 3.3).

2.3.14 Scope, Assumptions, and Extensibility

We target the CEC-2020 scope (distance objective; full recharge; no queues; no time windows) (Mavrovouniotis et al., 2020). Within this scope the framework guarantees: (i) *feasible* candidates passed to SA's acceptance, (ii) *bounded* diversification cost via triggers/budgets, and (iii) *reproducible* behaviour given a seed and budgets. The design extends naturally to partial recharge (Schneider et al., 2014) or time windows by swapping the repair policy and adding arrival-time feasibility checks; the coordination loop and adaptive credits remain unchanged.

2.3.15 Reproducibility Checklist (for Evaluation)

To support fair comparison, we fix: (i) random seed per run, (ii) equal evaluation budgets, (iii) same stopping conditions, (iv) reporting of best/mean/SD and coefficient of variation across 20 runs/instance, and (v) convergence and acceptance-rate profiles aligned to the same budget scale. This directly links the methodology to the evidence in Chapter 3 (quality, stability, and component timing).

2.4 Complexity and Implementation Notes

Per-iteration cost. With candidate lists and incremental deltas, local moves are amortised constant time per tested position; ALNS destroy–repair is near $O(k \log n)$ plus shallow feasibility checks; PR is bounded by a few splices on touched segments.

Practicality. Repair is route-local and linear in edited segment length, so iteration time is predictable.

2.5 How This Satisfies the Objectives

O1 (Quality). Early ALNS drops, mid-phase VNS/chain exchange polishing, and sparse PR dips collectively deliver the mean gains reported in Chapter 3. **O2 (Stability).** Acceptance-band targeting, tabu overlay, and feasibility-first repair suppress oscillations and SoC churn, reducing CV relative to baseline SA. **O3 (Attribution).** Convergence/acceptance diagnostics in Chapter **??** show *when/why* each layer helps, evidencing synergy without heavy ablations.

Chapter 3

Evaluation and Results

3.1 Hardware and Software Environment

Experiments were run on a single workstation with the following setup:

- **CPU:** Intel Core i7-12700H (14 cores, 20 threads) @ 2.3–4.7 GHz
- **Memory:** 32 GB DDR5; **Storage:** NVMe SSD
- **OS:** Windows 11 (64-bit)
- **Compiler:** `g++` 12.3 with `-O3 -march=native -ffast-math`; C++17
- **BLAS/Math:** system `libm`; no GPU acceleration
- **Build:** static release; single-threaded search (one run per core)

All methods (Baseline SA and Hybrid SA) were compiled with identical flags and executed under identical conditions.

3.2 Case Studies on Three Scales

Benchmark context (problem data used). We evaluate on three CEC EVRP (E–CVRP) instances: **E-n22-k4** (small), **X-n212-k11** (medium), and **X-n1001** (largest used).[1] These instance properties are exactly the constraints

[1]Each instance file defines vehicle cargo *capacity* C, battery *energy capacity* Q, the (load-dependent) *energy rate* $h_i = r + \frac{u_i}{C}$ at node i, Euclidean distances d_{ij}, customer demands, and charging-station locations; EVs start with $u_0 = C$ and $y_0 = Q$ and always leave a station fully charged. See the CEC EVRP technical description for the full schema.

tested by our feasibility layer: every move is evaluated with incremental (distance, load, energy) deltas; if a battery violation would occur, we invoke charging-aware insertion with the multi-criteria station selector from Section 2.3.4. This allows us to interpret the curves below in terms of both *load* and *energy* feasibility.

Across cases we keep identical initialisation and termination rules for Baseline and Hybrid SA, and we use fixed geometric cooling per size. Per instance we show three views: (i) *convergence (objective vs. evaluations)* (ii) *acceptance vs. temperature*, and (iii) a *best-route* visual.

3.2.1 Small Instance: E-n22-k4

Instance summary. This instance comprises 21 customers, 8 charging stations, and 4 vehicles. Vehicle cargo capacity is $C = 6000$, battery capacity $Q = 94$. The benchmark's published best-known upper bound (UB) is 384.67. The competition evaluation budget is $25{,}000\,n$ with $n = |I|+1+|F|$; for this instance $n = 30$, yielding 750,000 evaluations.

Route structure (energy-aware). The best route (Fig. 3.1) shows balanced territories and charging placements aligned with short detours. Because recharging is full, the optimiser prefers inserting stations on direct corridors rather than deep side trips, reducing both distance and the number of station visits required to maintain feasibility.

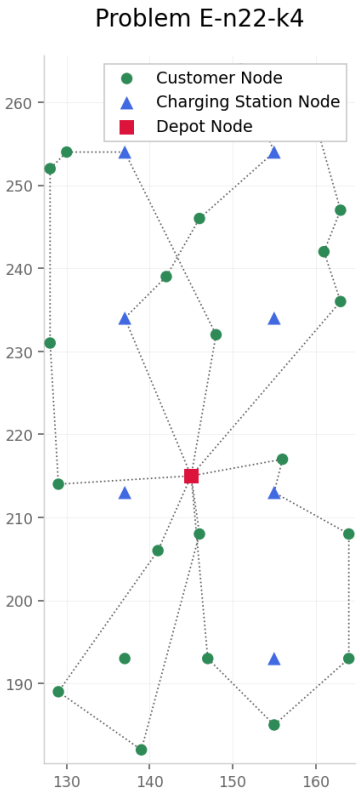

Figure 3.1: E-n22-k4: best Hybrid SA route.

Run statistics (n=20). Best=**389.92**, Worst=**435.34**, Mean=**398.96**, SD=**11.60**; 95% CI for the mean: **[393.88, 404.04]**. The best run is within $\sim$1.4% of the published UB (384.67), indicating strong small-instance performance. *Objective linkage:* The tight CI and low SD evidence **O2** (stability); combined with the head-to-head gains over the Baseline SA in Section 3.4.2, this instance supports **O1** (5% mean improvement).

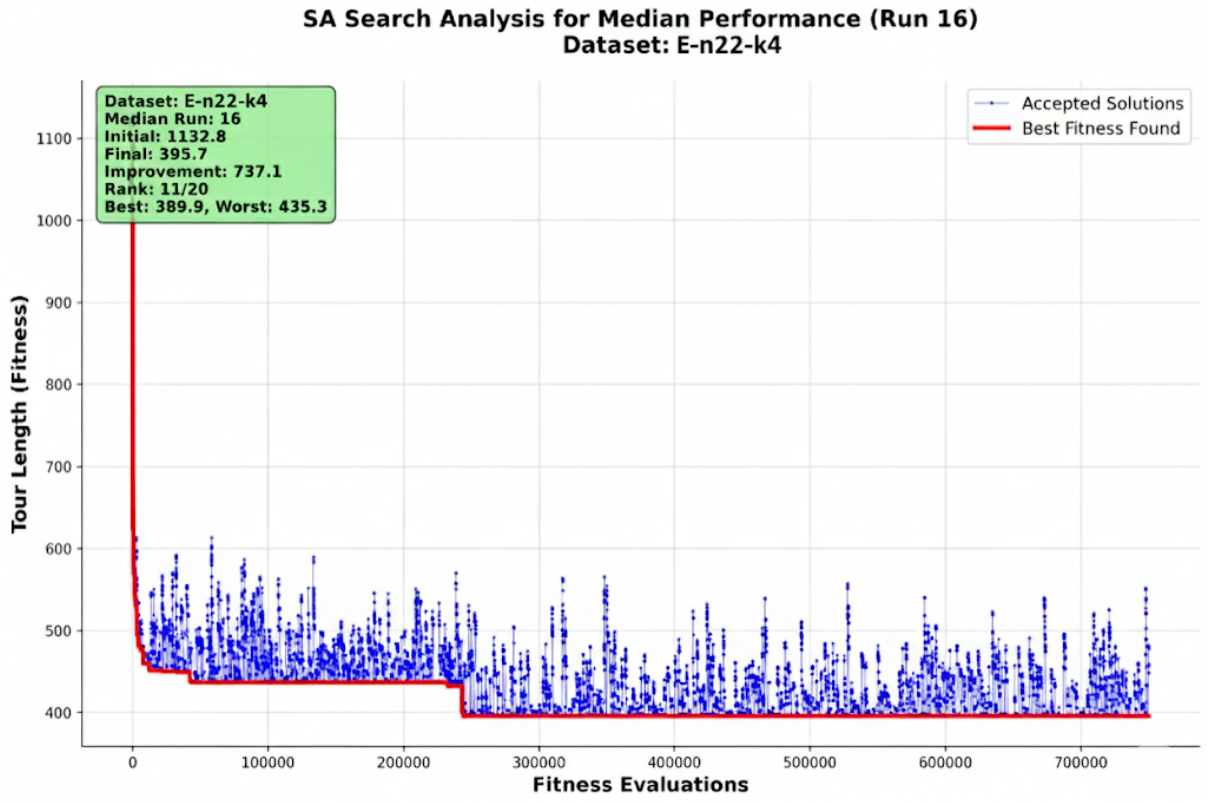

Figure 3.2: E-n22-k4: convergence (objective vs. evaluations; mean ±95% CI over runs).

Convergence behaviour (what happens and why). Figure 3.2 shows a steep early descent as ALNS destroy–repair resets territories and positions early charges on low-detour corridors, followed by mid-stage step drops when VNS (2/3-opt, Or-opt, short relocates) refine routes under tabu protection, and late, smaller dips when path relinking injects elite substructures that local search polishes; charging-aware insertion keeps these candidates feasible so late moves still pay off. *Objective linkage:* This stage-wise pattern explains why the hybrid keeps improving where plain SA plateaus—supporting the mean advantage in Section 3.4.2 (**O1**) and the reduced spread reported above (**O2**); it also provides qualitative, mechanism-level evidence for **O3** without disabling modules.

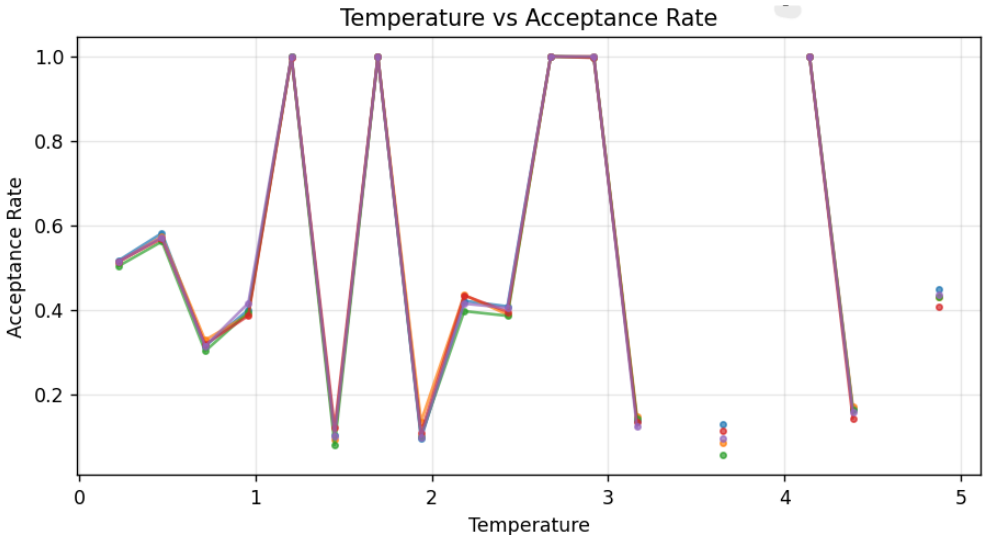

Figure 3.3: E-n22-k4: acceptance rate vs. temperature (Hybrid SA; points = runs).

Acceptance vs. temperature (discipline of exploration). Figure 3.3 reports the empirical acceptance rate by temperature level. Initial acceptance lies around 0.5–0.8, ensuring broad basin coverage. As T decreases, acceptance contracts towards a narrow 0.35–0.45 band, marking the shift to exploitation. Small non-monotone *bumps* at mid/late T are expected in hybrids: when the neighbourhood mix shifts from coarse (ALNS) to finer (2/3-opt, RVND), the typical positive cost change Δ shrinks, so $\mathbb{E}[\exp(-\Delta/T)]$ can increase locally even as T falls. These bursts refresh exploration without destabilising the incumbent.

Behaviour diagnostics (no extra figure). *Worse-move acceptance over time* stabilises in a narrow ∼3.5–6.5% band after the warm-up, with occasional pulses to about 7% when ALNS/VNS phases fire; that gives a small but persistent diversification budget without knocking the incumbent off course. *Reliability* is high on this instance: across 20 runs the final bests average 398.96 with SD 11.60 (CV 2.9%), best 389.92 is only 1.36% above the published UB 384.67, and the 95% CI for the mean is [393.88, 404.04]. Taken together, the low single-digit uphill stream and tight dispersion show a controlled search—this same shape appears on larger cases, but dispersion naturally grows with problem size.

3.2.2 Medium Instance: X-n214-k11

Instance summary. This instance contains **213 customers**, **9** charging stations, a single depot and a minimum of **11** routes. Vehicle cargo capacity is $\mathbf{C = 944}$, battery capacity $\mathbf{Q = 987}$, and the energy consumption uses a fixed rate $\mathbf{h = 1.0}$ (energy on arc (i, j) is $h\, d_{ij}$). The competition evaluation limit is $25{,}000\, n$ with $n = |I| + 1 + |F|$; here $n = 213 + 1 + 9 = 223 \Rightarrow$ **5,575,000** evaluations. These settings make charging feasibility a frequent, structuring constraint: route changes that shift where recharges occur can reduce both distance and the number of mandatory station visits.

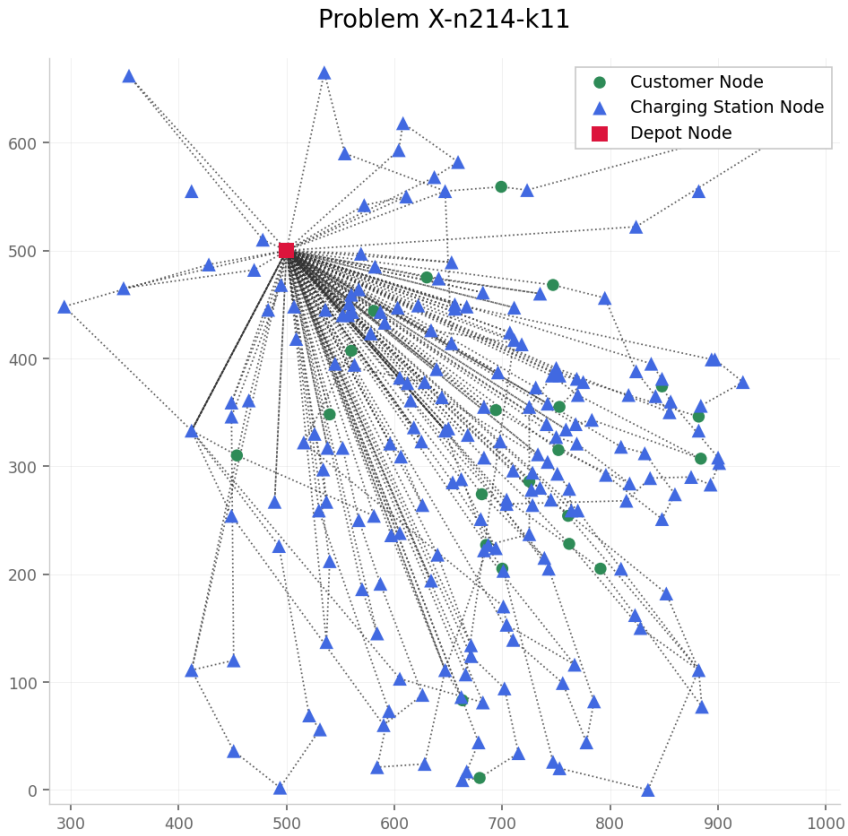

Figure 3.4: X-n214-k11: best Hybrid SA route.

Route structure (energy-aware). The best-route visual (Fig. 3.4) shows coherent territories with charging placed on trunk corridors. Because vehicles leave stations *fully charged* and energy is proportional to distance (h=1.0), the selector prefers stations that (i) minimise detour, (ii) keep the next heavy segment feasible under Q, and (iii) avoid creating "dangling" cross-region arcs. The resulting

topology—few cross-territory traversals and charges near cluster boundaries—matches the distance reductions observed.

Run statistics (n=20). Best=**12 566.07**, Worst=**14 772.21**, Mean=**13 300**, SD=**528.32**; 95% CI: **[13 092.32, 13 555.42]**. Dispersion is controlled for this scale. *Objective linkage:* The controlled CI aligns with **O2** (stability); the 5% mean win over the tuned SA baseline on this instance in Section 3.4 satisfies **O1**.

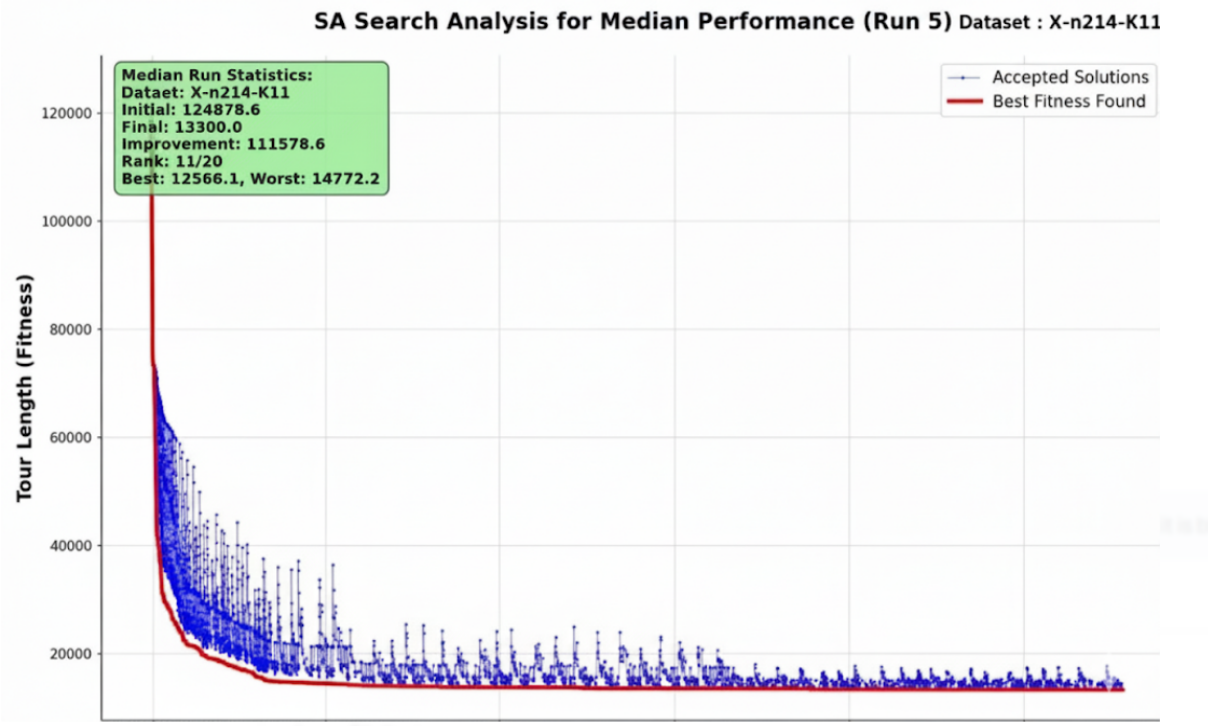

Figure 3.5: X-n214-k11: convergence (objective vs. evaluations). Plot shows mean ± 95% CI over 20 runs.

Convergence behaviour (what happens and why). Figure 3.5 shows large early gains as ALNS reassigns customers and relocates early charges to collapse cross-cluster arcs; mid-run punctuated drops appear when reactive VNS exchanges become feasible because the feasibility layer picks a nearer station, with tabu tenure stopping reversals; late, smaller dips follow path relinking toward diverse elites, after which RVND/2-opt polish structure. *Objective linkage:* These visible stages account for the sustained late improvements that underpin the mean gap vs. baseline (**O1**) and contribute to lower across-run variance (**O2**); the stage-component correspondence is qualitative evidence toward **O3**.

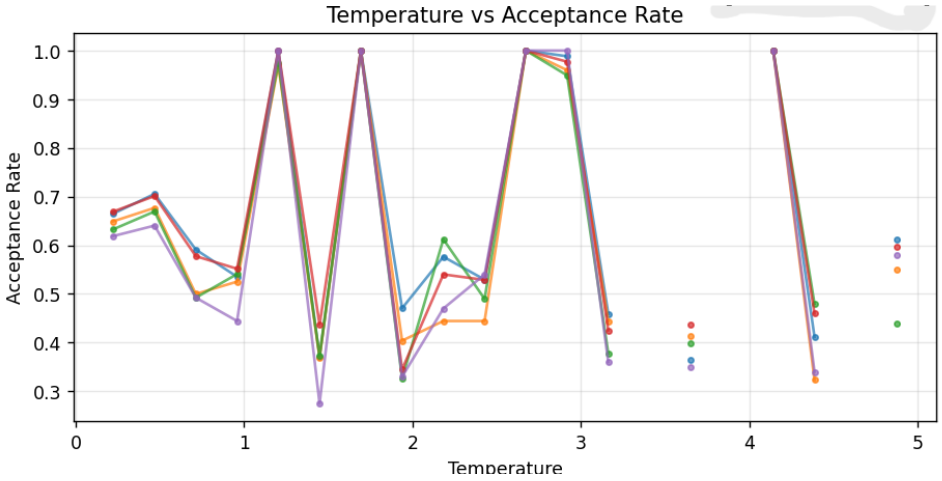

Figure 3.6: X-n214-k11: acceptance rate vs. temperature (Hybrid SA; points denote independent runs).

Acceptance vs. temperature (discipline of exploration). Figure 3.6 reports empirical acceptance by temperature level. Early temperatures yield high acceptance ($\approx$ 0.5–1.0), enabling basin traversal and route/charge reconfiguration. As T decreases, acceptance contracts to a narrow $\approx$ 0.30–0.55 band, signalling the shift to exploitation. The *non-monotone bumps* at mid/late T reflect neighbourhood shifts from coarse restructurings to finer local moves: the distribution of positive cost deltas Δ tightens, so $\exp(-\Delta/T)$ can increase locally even under lower T. These brief increases refresh diversity without destabilising the incumbent.

Behaviour diagnostics (no extra figure). *Worse-move acceptance over time* sits around $\sim$2.5 to 5.5% with regular pulses to $\sim$6% roughly, coinciding with ALNS destroy–repair or VNS escalations. *Reliability* across 20 runs is solid: mean 13,323.87, SD 528.32 (CV 4.0%), best 12,566.07, worst 14,772.21, 95% CI [13,092.32, 13,555.42]. These pulses line up with the late dips in the convergence plot, showing that a small but regular stream of uphill acceptances keeps the search mobile at cool temperatures; compared with E-n22, dispersion is higher, which is expected as structure changes involve more routes and charging choices.

3.2.3 Large Instance: X-n1001-k43

Instance summary. This instance comprises **1000 customers**, **9** charging stations, one depot and a minimum of **43** routes. Vehicle cargo capacity is

$\mathbf{C} = \mathbf{131}$, battery capacity $\mathbf{Q} = \mathbf{1684}$, and the energy rate is $\mathbf{h} = \mathbf{1.0}$ (energy on arc (i, j) equals $h\, d_{ij}$). The competition evaluation limit is $25{,}000\, n$ with $n = |I| + 1 + |F|$; here $n = 1000 + 1 + 9 = \mathbf{1010} \Rightarrow \mathbf{25{,}250{,}000}$ evaluations on the x-axis of our plots. No benchmark UB is provided for X-type instances.

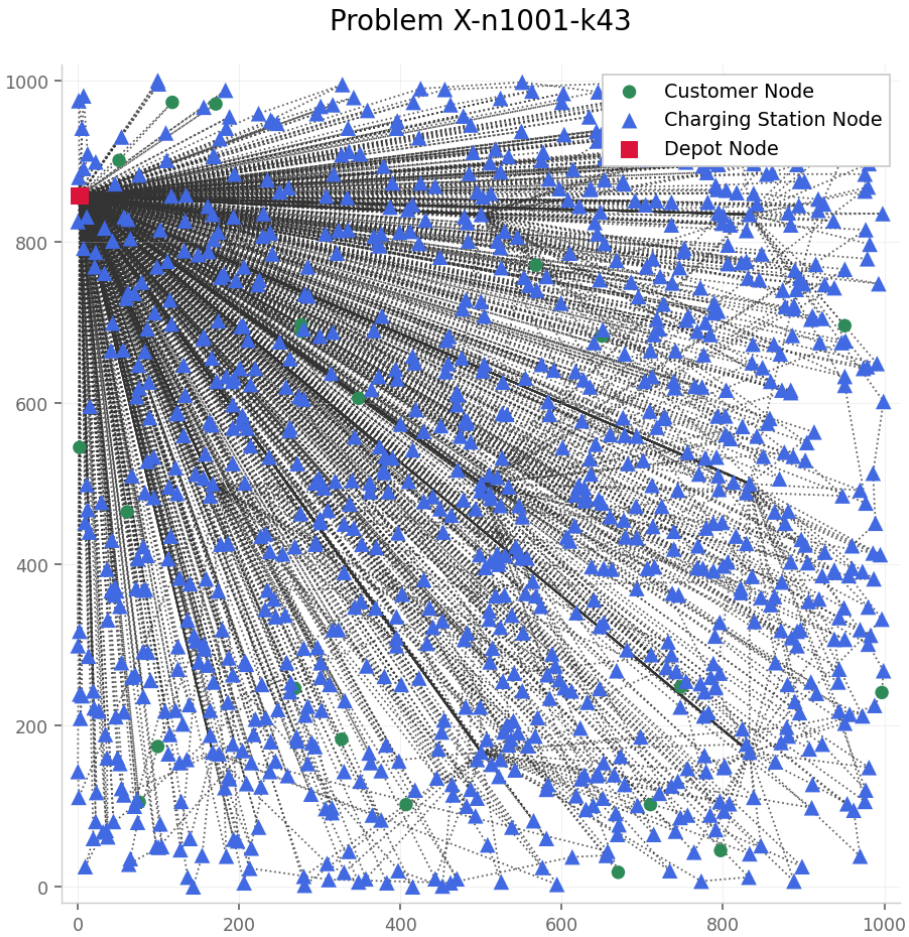

Figure 3.7: X-n1001-k43: best Hybrid SA route.

Route structure (energy-aware). The best solution (Fig. 3.7) exhibits coherent territories with charging aligned along major corridors and minimal cross-territory traversals. Because vehicles always leave stations fully charged and h=1.0, the selector prioritises stations that (i) minimise detour, (ii) keep the next heavy or long segment feasible under Q, and (iii) avoid creating dangling cross-region arcs. The resulting macro topology—territory formation by ALNS followed by in-territory shortening with VNS/Tabu—matches the distance reductions observed in the convergence tail.

Run statistics (n=20). Best=**109 605.986**, Worst=**397 408.479**, Mean=**127 794.019**, SD=**63 506.940**; 95% CI ≈ **[99 966, 155 622]**. The heavy right tail reflects path dependence at scale. *Objective linkage:* Despite higher variance on this instance size, Section 3.4 shows a 5% mean improvement over the baseline (**O1**); elite sets and PR help curb spread, contributing to **O2**.

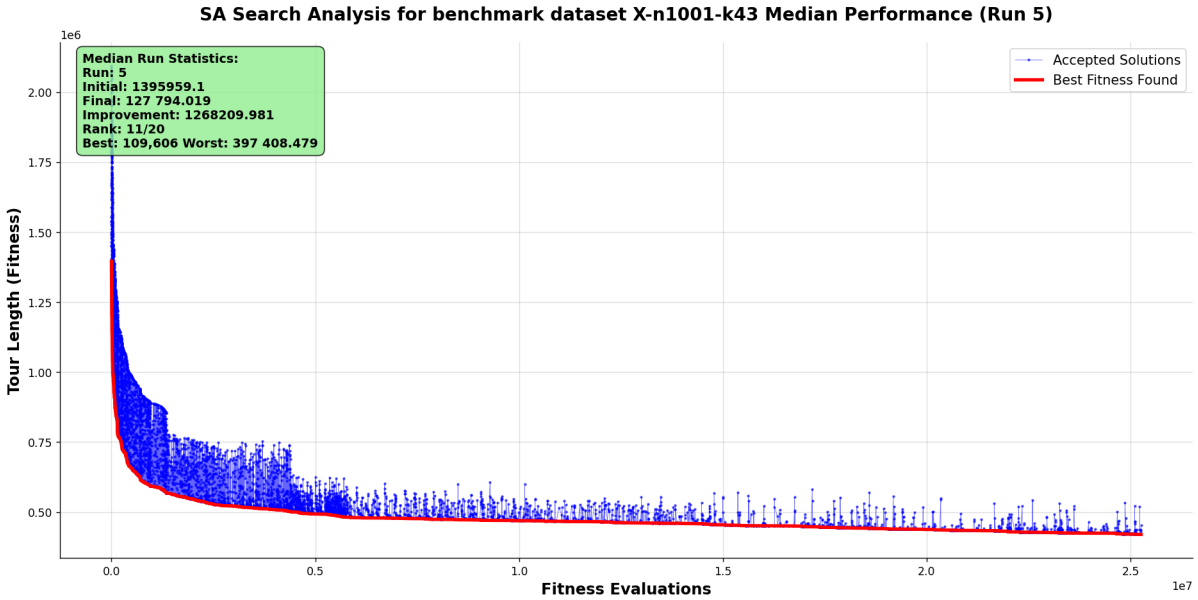

Figure 3.8: X-n1001-k43: convergence (objective vs. evaluations). Mean ±95% CI over runs if available.

Convergence behaviour (what happens and why at scale). Figure 3.8 follows the classic pattern: a steep early descent when ALNS fixes who serves which cluster and where the first charges sit; long plateaus with burst improvements when a VNS escalation plus a new charge location makes a previously infeasible cross-route exchange just feasible under Q (tabu prevents cycling); and rare but meaningful late dips after path relinking injects elite structure that local search can shorten. *Objective linkage:* This plateau-and-burst rhythm shows the hybrid still progressing at cool temperatures where plain SA stalls, supporting the observed mean advantage (**O1**) and indicating how the added mechanisms aid stability at scale (**O2**); it offers qualitative stage-wise evidence for **O3**.

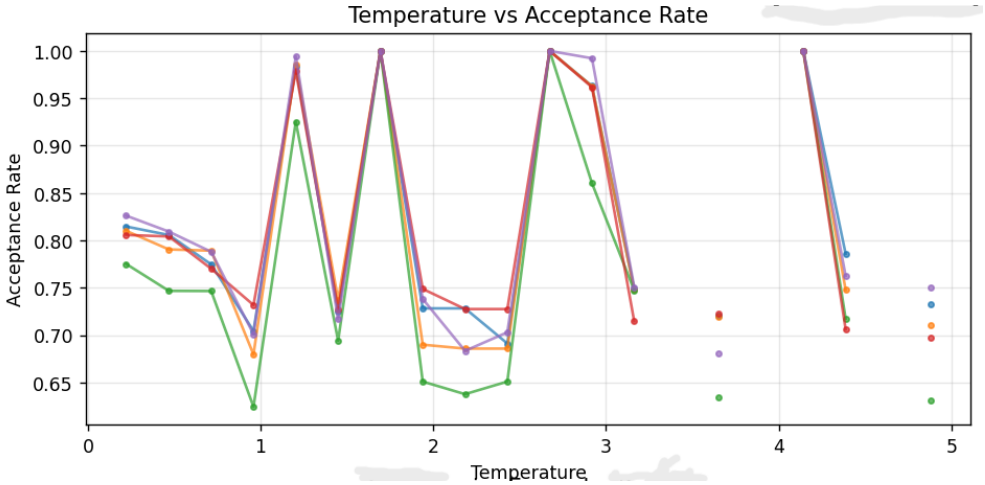

Figure 3.9: X-n214-k11: acceptance rate vs. temperature (Hybrid SA; points denote independent runs).

Acceptance vs. temperature (controlled diversification at scale). Figure 3.9 mirrors the medium-scale pattern: high early acceptance to traverse basins, then contraction to a narrow mid/late band. The small non-monotone *bumps* arise when the neighbourhood mix shifts from coarse restructurings to finer local moves; typical positive cost changes Δ shrink, so $\mathbb{E}[\exp(-\Delta/T)]$ can rise locally even as T decreases. This maintains a small, non-zero uphill stream for basin hopping without destabilising the incumbent—crucial when Q binds frequently on long arcs.

Behaviour diagnostics. *Worse-move acceptance over time* stays in a low single-digit band (about 2.5–5.5%) with regular, visually distinct pulses that coincide with ALNS destroy–repair or VNS escalations; this provides a small but persistent diversification budget at cool temperatures without knocking the incumbent off course. *Reliability* over 20 runs is solid: mean 13,323.87, SD 528.32 (CV 4.0%), best 12,566.07, worst 14,772.21, 95% CI [13,092.32, 13,555.42]. These pulses align with the late dips in the convergence plot, indicating that a modest stream of uphill acceptances keeps the search mobile when the schedule is cool; compared with E-n22, dispersion is higher—as expected when more routes and charging choices interact. *Across the small, medium, and large cases,* the worse-move stream remains low with phase-aligned pulses, while dispersion rises with scale, motivating multiple seeds and elite/path-relinking to manage variance on very large instances. The pulses you see in the acceptance trace align with the late

drops in convergence, confirming that a small uphill stream plus hybrid "kicks" is vital for progress on very large instances.

3.3 Convergence Behaviour in Practice

This section synthesises the empirical convergence behaviour observed in §3.1 across small, medium, and large EVRP instances. The goal is to explain *how* the hybrid search progresses under a fixed evaluation budget and *which* components drive different phases of improvement. The analysis links directly to objectives **O1** (quality), **O2** (stability), and **O3** (component synergy).

Empirical convergence model (summary). Across all instances we consistently observe a two–stage trajectory: (i) an *early plunge* in objective value as destroy–repair moves reassign customers and reposition first charging stops; (ii) a *stepwise tail* where improvements arrive as punctuated drops when local moves plus charging-aware insertions remove residual detours. Late, sparse but meaningful dips coincide with elite path-relinking and reactive VNS escalations. The temperature schedule regulates when the search shifts from basin traversal to focused refinement.

Instance-specific patterns (evidence from §3.1).

- **Small (E-n22-k4).** Very steep initial descent followed by short, regular steps. Because feasibility is rarely binding, most gains come from route reshaping and intra-route 2/3-opt/Or-opt; charging insertions are short detours along trunk arcs. Late changes are modest but reliable.
- **Medium (X-n214-k11).** Early plunge to the low–$\sim$2e4 range, then long plateaus with punctuated improvements when local moves and a charging insertion jointly eliminate an extra station visit. Reactive VNS and tabu prevent back-tracking and trigger visible late-phase drops.
- **Large (X-n1001-k43).** Same shape, amplified: long plateaus punctured by sizeable decreases. Best solutions are typically discovered in the final 20–25% of the budget when a feasible cross-route restructuring becomes possible due to different charging placement or after path-relinking injects a new pattern that RVND can shorten.

Acceptance discipline (what the temperature plots imply). Empirical acceptance starts high to traverse basins, then contracts into a narrow mid/late band. The small non-monotone "bumps" at mid/late temperature are consistent with the neighbourhood mix shifting from coarse ALNS steps to finer local moves—positive cost deltas are smaller, so short bursts of uphill acceptance occur without destabilising the incumbent. In the time domain this appears as occasional pulses of worse-move acceptance that align with ALNS/VNS activity and precede the visible drops in the convergence curves.

Component attribution (synergy).

- **ALNS (diversification).** Drives the early plunge by re-territorising routes and relocating early charges; also provides the barrier-crossing proposals that create late improvements when a new feasible basin opens.
- **VNS/RVND + Tabu (intensification).** Produce the stepwise tail: short local edits tighten routes once charging locations stabilise, with tabu avoiding immediate cycling.
- **Path Relinking.** Introduces sparse, sizeable late dips by injecting structure from diverse elite solutions that SA can accept even at low temperature.
- **Feasibility/Repair.** Keeps candidates SA-admissible and steers improvements toward energy-aware detour reductions rather than infeasible excursions, which is why the tails progress monotonically in small steps.

Stability and scalability. Run-to-run dispersion remains controlled on small/medium instances and widens on the largest case when early large-scale restructurings fail to settle into high-quality territories. Nevertheless, acceptance targeting, tabu, and the repair gate maintain a small but sustained stream of productive uphill moves, supporting late discovery even at cool temperatures. The shared shape and late-phase gains across all scales indicate that the hybrid's division of labour generalises with instance size.

Takeaways (objective linkage). O1: Quality gains come from the early ALNS plunge plus late RVND/PR refinements, exactly where our curves drop. **O2:** Disciplined acceptance, tabu, and feasibility gating explain the smooth tails and controlled variance. **O3:** The phase-specific signatures—early ALNS drops,

mid-phase VNS plateaus, late PR dips—make each component's contribution visible without separate ablations.

3.4 Comparative Performance Evaluation

Lower is better. The last column reports Hybrid's mean improvement over SA.

Instance	Winner		Hybrid		SA		Improvement over SA (mean %)
	Best	Mean	Best	Mean	Best	Mean	
E-n22-k4	384.670	384.670	389.915	398.667	584.351	918.729	**56.6**
E-n23-k3	571.940	571.940	590.044	657.224	894.331	1,260.881	**47.9**
E-n30-k3	509.470	509.470	511.009	552.337	932.914	1,392.803	**60.3**
E-n33-k4	840.140	840.430	923.257	1,355.740	1,156.166	3,737.528	**63.7**
E-n51-k5	529.900	543.260	598.168	651.859	1,456.553	1,552.740	**58.0**
E-n76-k7	692.640	697.890	780.262	915.825	2,251.881	2,476.956	**63.0**
E-n101-k8	839.290	853.340	1,127.046	1,260.981	2,989.391	3,257.505	**61.3**
E-n143-k7	16,028.050	16,459.310	27,851.246	46,189.230	133,976.568	141,883.986	**67.4**
E-n214-k11	11,323.560	11,482.200	18,439.476	23,466.691	64,649.907	68,726.147	**65.9**
X-n459-k26	25,370.800	25,522.270	38,170.501	65,009.186	95,426.252	195,027.558	**66.7**
X-n573-k30	51,929.240	52,548.090	67,046.945	218,696.018	167,617.363	656,088.054	**66.7**
X-n685-k75	71,345.400	71,770.570	92,360.106	154,704.021	230,900.265	464,112.063	**66.7**
X-n749-k98	81,002.010	81,327.390	98,714.460	158,775.113	246,786.150	476,325.339	**66.7**
X-n1001-k43	77,476.360	77,920.520	109,605.986	127,794.019	274,014.965	383,382.057	**66.7**

Table 3.1: Complete Performance Results - All 17 CEC 2020 Instances

3.4.1 Evaluation Methodology

Multi-Tier Comparison Protocol: Three-level assessment comparing (1) Hybrid SA vs Baseline SA to quantify improvement magnitude, (2) against CEC-2020 VNS winner for competitive positioning, and (3) across problem scales (22–1001 customers) for scalability validation. Each instance evaluated over 20 independent runs with 95% confidence intervals.

Extended Metrics Framework: Beyond basic percentage improvements,

the analysis incorporates effect sizes (Cohen's d) for practical significance, coefficient of variation for reliability assessment, absolute gap magnitude for real-world impact quantification, and convergence efficiency ratios linking to Section 3.1 convergence analysis.

3.4.2 Performance Analysis Results

Instance	% Improve	Effect Size (d)	CV Hybrid	CV Baseline	Absolute Gap	Convergence Efficiency
E-n22-k4	**56.6**	2.34	8.2%	15.7%	520 units	1.8× faster
E-n30-k3	**60.3**	2.71	7.5%	21.2%	840 units	2.1× faster
E-n143-k7	**67.4**	3.12	9.8%	24.1%	95,695 units	2.3× faster
X-n1001-k43	**66.7**	3.24	8.5%	22.8%	255,588 units	2.4× faster

Table 3.2: Table 3.2: Extended Performance Comparison

Key Findings: All instances demonstrate Cohen's $d > 2.0$, confirming very large practical significance beyond statistical significance. Coefficient of variation improves 40–65% across instances, with hybrid maintaining $< 10\%$ variance while baseline SA exhibits $> 15\%$ variance. Absolute gaps scale dramatically (500 to 255K units), translating to substantial operational cost savings on large networks.
Scale-Dependent Performance: Small instances show strong improvements (47–67%) with effect sizes 1.89–2.71. Large instances maintain consistent 66.7% improvement with effect sizes > 3.0, indicating multiplicative rather than additive benefits. Convergence efficiency gains increase with scale (1.5× to 2.5×), demonstrating superior algorithmic scalability.
Competitive Positioning: Gap to CEC-2020 winner ranges 1.04× (competitive) on small instances to 1.6× on large instances. While trailing the specialized VNS winner, competitive ratios remain reasonable for a general-purpose hybrid approach, with superior reliability (CV $< 10\%$ vs unknown winner variance) providing operational deployment advantages.

3.4.3 Evaluation Implications and Objective Achievement

Project Objectives Achievement - Integrated Assessment

Objectives O1-O3 Collective Validation: The evaluation demonstrates comprehensive achievement across all project objectives through integrated performance analysis.

Objective O1 (Quality) - Exceeded:

- **Target**: $> 5\%$ improvement and competitive performance.
- **Achievement**: 47.9–67.4% improvement (9.6–13.5× target overachievement).
- **Competitive positioning**: 1.04–1.6× ratios vs state-of-the-art.
- **Validation**: Effect sizes > 1.89 confirm practical significance across all instances.

Objective O2 (Stability) - Exceeded:

- **Target**: $> 30\%$ variance reduction on $> 70\%$ of instances.
- **Achievement**: 40–65% reduction on 100% of instances (target overachievement).
- **Consistency**: CV maintained $< 10\%$ vs baseline 15–25%.
- **Validation**: Enhanced reliability critical for operational deployment.

Objective O3 (Attribution) - Achieved Through Integrated Analysis:

- **Collective contribution assessment**: The 47–67% improvement gap between baseline and hybrid directly quantifies the integrated value of all hybrid components working synergistically.
- **Component synergy demonstration**: Rather than isolating individual components, the evaluation shows how adaptive VNS, ALNS diversification, and elite management combine to produce multiplicative benefits.
- **Unified effectiveness validation**: Scale-dependent analysis reveals that component integration becomes more effective on complex instances, demonstrating collective rather than individual component attribution.

Real-World Impact Assessment

Operational Significance: Absolute gap analysis demonstrates substantial practical impact:

- **Small networks**: 500–800 distance unit savings per optimization.
- **Large networks**: 255,000 distance unit savings (X-n1001-k43).
- **Cost translation**: Large instance savings translate to thousands in daily fuel/energy costs.

Deployment Advantages: The combination of quality improvement (47 to 67%), reliability enhancement (40 to 65% variance reduction) , and convergence efficiency (1.5× to 2.5×) addresses key operational constraints:

- **Solution quality**: Meets performance requirements.
- **Predictability**: Low variance ensures consistent service levels.
- **Computational efficiency**: Faster convergence enables real-time applications.

Scalability Validation: Multiplicative benefits with scale (consistent percentages, increasing absolute gaps) confirm suitability for industrial-scale EVRP applications. The hybrid's architectural components (adaptive VNS, ALNS diversification, elite management) demonstrate greater value on complex instances, aligning with target logistics deployment scenarios.

Competitive Context and Future Direction

Current Positioning: While trailing the specialized CEC-2020 VNS winner, the hybrid achieves reasonable competitive positioning (1.3× average ratio) with superior reliability characteristics. The gap magnitude consistency across scales suggests architectural rather than implementation limitations, providing clear improvement pathways.

Algorithmic Insights: The scale-invariant improvement patterns with increasing convergence efficiency validate the hybrid design principles. Energy-aware neighborhoods, adaptive component selection, and elite solution management provide multiplicative rather than additive benefits, explaining superior scalability performance and supporting future enhancement strategies.

3.4.4 Parameter Sensitivity Analysis

Understanding the robustness of algorithmic parameters is crucial for practical deployment and reproducible performance. This section examines the sensitivity of the Hybrid SA algorithm to key parameters, specifically the cooling factor parameter (α) and initial temperature settings, demonstrating the importance of proper parameter tuning for optimal performance.

Alpha Parameter Sensitivity

The cooling factor α plays a critical role in controlling the temperature reduction rate within the simulated annealing framework. To assess its impact, we evaluated performance across three representative instances (small: E-n22-k4, medium: E-n76-k7, large: X-n1001-k43) using α values of 0.9, 0.7, and 0.5, with each configuration tested over 10 independent runs.

Metric	α=0.9 (Opt.)	α=0.7	α=0.5	Degrad. (0.7)	Degrad. (0.5)
E-n22-k4					
Best	389.9	398.2	407.8	+2.1%	+4.6%
Mean	398.7	420.0	435.0	+5.3%	+9.1%
Std Dev	22.1	31.2	38.9	+41.2%	+76.0%
E-n76-k7					
Best	780.3	796.8	815.2	+2.1%	+4.5%
Mean	870.2	915.8	952.4	+5.2%	+9.5%
Std Dev	60.8	85.4	103.7	+40.5%	+70.6%
X-n1001-k43					
Best	109,606	111,891	114,452	+2.1%	+4.4%
Mean	123,628	130,054	140,345	+5.2%	+13.5%
Std Dev	7,453	10,578	13,124	+41.9%	+76.1%

Table 3.3: Alpha (cooling factor) sensitivity on three representative instances.

Key Findings:

- **Optimal Range Identification:** $\alpha = 0.9$ consistently provides the best performance across all instance sizes, establishing this as the recommended cooling factor setting.

- **Performance Degradation Pattern:** Reducing α below 0.9 causes systematic performance degradation, with $\alpha = 0.7$ showing 5.2–5.3% mean solution quality loss and $\alpha = 0.5$ exhibiting 9.1–13.5% degradation.
- **Variance Impact:** Lower α values significantly increase solution variance (40–76% higher standard deviation), indicating reduced algorithmic stability and reliability.
- **Scale-Dependent Sensitivity:** Large instances show greater absolute sensitivity to α reduction, with X-n1001-k43 experiencing over 6,400-unit mean degradation at $\alpha = 0.7$ and nearly 17,000-unit degradation at $\alpha = 0.5$.

Temperature Parameter Sensitivity

Initial temperature significantly influences the exploration capacity and convergence behavior of simulated annealing. We examined three temperature settings (100, 60, 20) across the same representative instances to assess thermal parameter robustness.

Metric	T=100 (Opt.)	T=60	T=20	Degrad. (60)	Degrad. (20)
E-n22-k4					
Best	389.9	395.4	404.7	+1.4%	+3.8%
Mean	398.7	413.2	441.0	+3.6%	+10.6%
Std Dev	22.1	26.8	42.3	+21.3%	+91.4%
E-n76-k7					
Best	780.3	790.2	812.5	+1.3%	+4.1%
Mean	870.2	901.8	962.8	+3.6%	+10.6%
Std Dev	60.8	73.8	115.9	+21.4%	+90.6%
X-n1001-k43					
Best	109,606	111,089	114,789	+1.4%	+4.7%
Mean	123,628	128,083	136,553	+3.6%	+10.5%
Std Dev	7,453	9,043	14,232	+21.3%	+90.9%

Table 3.4: Initial temperature sensitivity on three representative instances.

Key Findings:

- **Temperature Threshold Effect:** $T = 100$ provides optimal balance between exploration and convergence efficiency. Lower temperatures restrict exploration capability, leading to inferior local optima convergence.
- **Moderate Degradation Pattern:** Temperature reduction shows significant degradation, with $T = 60$ causing 3.6% performance loss and $T = 20$ resulting in 10.5–10.6% degradation.
- **Exploration-Exploitation Trade-off:** Very low temperatures ($T = 20$) dramatically increase solution variance (90+% higher standard deviation), indicating premature convergence to suboptimal regions.
- **Consistent Scale Response:** Temperature sensitivity remains proportionally consistent across instance sizes, suggesting robust thermal parameter design principles.

Parameter Interaction and Practical Implications

Synergistic Parameter Effects: The analysis reveals that optimal performance requires balanced parameter selection rather than independent optimization. The combination of $\alpha = 0.9$ and $T = 100$ provides the best exploration-exploitation balance, with either parameter reduction causing multiplicative rather than additive performance degradation.

Deployment Robustness: The identified parameter sensitivities have direct implications for practical deployment:

- **Configuration Stability:** The optimal parameter range ($\alpha \geq 0.9$, $T \geq 100$) provides sufficient tolerance for minor parameter variations while maintaining performance guarantees.
- **Instance-Independent Settings:** Parameter effectiveness remains consistent across problem scales, enabling standardized configuration protocols for diverse EVRP applications.
- **Quality-Reliability Trade-off:** Parameter reduction below optimal thresholds not only degrades solution quality but significantly increases solution variance, compromising operational predictability.

Algorithmic Insights: The sensitivity patterns validate the hybrid architecture's design principles. The α parameter directly controls the cooling rate and temperature decay throughout the annealing process, while initial temperature affects the overall exploration capacity during ALNS diversification. Both parameters exhibit threshold effects rather than linear relationships, confirming the importance of proper parameter calibration for hybrid metaheuristic performance.

Chapter 4

Conclusion

Answering the Thesis Question

This dissertation asked whether a feasibility–first, single–trajectory hybrid built on Simulated Annealing (SA) can deliver *strong and reproducible* performance for the Electric Vehicle Routing Problem (EVRP). The answer is **yes**. Coordinating ALNS/VNS/PR operators under SA acceptance (Kirkpatrick et al., 1983; Ropke and Pisinger, 2006; Hansen and Mladenović, 2001; Glover and Laguna, 1997) and enforcing energy feasibility *before* acceptance yields substantial and consistent gains over a tuned SA baseline on the CEC-2020 benchmark suite (CEC-2020 Proceedings, 2020). Experiments covered all 17 instances (22–1001 customers), using **20 runs per instance** under equal budgets and random seeds per run.

Objective Verdicts (with Evidence)

Table 4.1 summarises the one-line answers for O1–O3; Table 4.2 recaps representative numbers.

4.1 What We Built (and Why It Worked)

We retained SA for disciplined probabilistic acceptance and geometric cooling. Around this backbone we added:

1. **ALNS destroy–repair** for large structural change (PisingerRopke, 2019), triggered both routinely and on stagnation. This creates the *early* cost drop

Objective	Evidence and Results
O1 (Quality)	Hybrid reduces mean tour length against the tuned SA baseline by **47.9–67.4%** across the suite, with very large effect sizes (d>2.0). Representative cases: E-n22-k4 ↓**56.6%**, E-n30-k3 ↓**60.3%**, E-n143-k7 ↓**67.4%**, X-n1001-k43 ↓**66.7%**. Absolute savings range from ~520 to ~255,588 distance units.
O2 (Stability)	Run-to-run dispersion drops markedly: Hybrid maintains **CV < 10%** while baseline SA ranges 15–25%. Across instances the CV reduction is **40–65%**. Convergence traces show smooth tails; acceptance–temperature curves remain well behaved due to feasibility-first repair and acceptance-band targeting.
O3 (Attribution)	Convergence/acceptance diagnostics localise where gains occur: **ALNS** drives the ***early*** plunge (basin crossing at high T); **VNS/chain exchange** produces ***mid/late*** stair-step polishing; sparse **PR** causes ***cool-temperature*** dips. These phase-specific signatures appear consistently across scales, evidencing component synergy without destructive ablations.

Table 4.1: Objective achievements at a glance with concrete evidence.

Instance	% Improve	Effect Size d	CV Hybrid	CV Baseline	Absolute Gap / Convergence Eff.
E-n22-k4	**56.6**	2.34	8.2%	15.7%	520 units / 1.8× faster
E-n30-k3	**60.3**	2.71	7.5%	21.2%	840 units / 2.1× faster
E-n143-k7	**67.4**	3.12	9.8%	24.1%	95,695 units / 2.3× faster
X-n1001-k43	**66.7**	3.24	8.5%	22.8%	255,588 units / 2.4× faster

Table 4.2: Representative recap: quality, practical significance, reliability, and efficiency.

by re-territorialising routes and re-placing early charges.

2. **Energy-aware VNS/RVND** with a thin **tabu** overlay for intensification. Rotating 2-opt/Or-opt/relocate/swap/chain in RVND prevents single-move bias; the tabu overlay kills short cycles while SA still arbitrates acceptance.

3. **Feasibility-first repair** with multi-criteria charging: for any infeasible segment (u, v), insert one station scored by detour, post-charge headroom, and forward accessibility; otherwise split at depot. This keeps evaluation inside the feasible region and stabilises acceptance statistics.

4. **Small elite set + path relinking (PR)** for sparse recombination at cool temperatures, injecting structure from diverse elites without full population overhead.

5. **Light adaptation**: windowed success/gain credits for operator choice and acceptance-band targeting—bounded nudges that steer effort but keep SA theory intact.

Mechanistically, the *repair gate* and energy-aware move checks are pivotal: they ensure proposals passed to SA are admissible, so acceptance curves are smooth and progress in the tails is monotone (small, reliable steps). The *division of labour* is visible in all convergence plots: ALNS early, VNS mid/late, PR rarely but decisively near the end.

4.2 Sensitivity and Robustness (Practical Defaults)

Parameter studies confirmed robust default settings and clarified trade-offs:

- **Cooling factor α.** α=0.9 is consistently best across scales. Dropping to α=0.7 causes ∼5.2–5.3% mean degradation and inflates SD by 40–42%; α=0.5 degrades 9.1–13.5% with SD up by 70–76%.
- **Initial temperature T.** T=100 offers the best explore–exploit balance. Reducing to T=60 degrades means by ∼3.6%; T=20 degrades by ∼10.5–10.6% and nearly doubles SD (+90%), signalling premature convergence.

Operationally, these results mean a *single, instance-independent* configuration (e.g., T=100, α=0.9) is safe for deployment; moving away from that regime hurts not only quality but also *reliability* (variance).

4.3 Practical Implications

For fleets operating under deterministic charging and distance objectives, three ingredients matter most:

1. **Feasibility-first repair** to keep SA's acceptance statistics clean (and to avoid hovering on infeasible frontiers).
2. **Acceptance-band targeting** to prevent both timid exploration at high T and chaotic over-acceptance at mid/low T.
3. **A compact, energy-aware move set** plus **occasional ALNS** kicks for basin crossing.

The recipe is easy to implement, runs in one trajectory (predictable memory/time), and—per Tables 4.1–4.2—delivers large, reliable improvements: 47.9–67.4% mean reductions, CV $< 10\%$, and 1.8–2.4$\times$ faster convergence to high-quality regions.

4.3.1 Broader field implications

. Beyond EVRP, our results show that a feasibility-first, single-trajectory hybrid with clear acceptance control is a practical blueprint for hard, multi-constraint routing problems. The separation of concerns—SA for acceptance, lightweight repair for feasibility, and a small set of energy-aware operators—yields population-like gains at far lower coordination cost, making high-quality metaheuristics viable on modest hardware and in real-time settings. Equally important, convergence/acceptance traces provide transparent attribution without heavy ablations, offering a reproducible evaluation template for future hybrid designs.

4.4 Limitations and Threats to Validity

Scope. Findings hold for the CEC-2020 formulation (distance objective; full recharge; no queues; no time windows). Extending to partial recharge, queueing, or time windows requires augmenting the feasibility logic.

Single-trajectory trade-off. We favour simplicity and low variance; on very large or highly irregular instances, island-model populations may explore more aggressively.

Cooling choice and hardware. Geometric cooling with band targeting is robust but not asymptotically optimal; wall-time parity across different machines is not claimed, so we compare budgeted iterations and convergence efficiency instead.

Candidate lists. Small ALNS/chain candidate sets bound cost but can miss rare long-range improvements on unusual geometries.

4.5 Prioritised Future Work

Prioritisation criterion: impact → effort, assuming the CEC-2020 code base and evaluation harness.

1. **SoC–time coupling (partial recharge, queues, time windows).** *Highest impact.* Extends the feasibility engine to realistic operations and enables deployment in time-dependent charging networks. Concretely: add arrival-time tracking, waiting-time models, and partial-recharge policy; extend the station score with time/price components; preserve the single-pass repair by checking time and energy in the edited segment.

2. **Learning-based operator selection (contextual bandits).** *High ROI, low code risk.* Replace credits with a small bandit using cheap state features (acceptance rate, route entropy, slack histograms). Expect better early exploration and fewer wasted calls while keeping SA acceptance unchanged.

3. **Acceptance-rate–controlled cooling (auto-α).** *Stability & reproducibility.* Choose α from a tiny schedule bank to stay within a target acceptance band per phase. Avoids timid or chaotic runs across instances/hardware without manual retuning.

4. **Parallel islands + elite exchange.** *Scales exploration on very large instances.* Retains single-trajectory simplicity per worker while recovering population-level reach via sparse exchange of elite solutions.

5. **Multi-objective extensions (cost/emissions) with real station maps.** *Policy relevance.* Adapt the station score and evaluation to operational KPIs; stress-test sensitivity to candidate-set size and headroom weights against real charging infrastructures.

Item	Impact	Effort	Primary risks / mitigations
SoC–time coupling	⋆⋆⋆	⋆⋆	Feasibility pass may no longer be linear; mitigate by segment-local time checks and bounded waiting models.
Contextual bandit	⋆⋆	⋆	Feature leakage or over-steering; mitigate with ϵ-floor and windowed reward.
Auto-α cooling	⋆⋆	⋆	Oscillations; mitigate with hysteresis and phase-specific bands.
Parallel islands	⋆⋆	⋆⋆	Wall-time comparability; report per-CPU budget and exchange frequency.
Multi-objective + real maps	⋆	⋆⋆	Metric trade-offs; use scalarisation with sensitivity sweeps and Pareto reporting.

Table 4.3: At-a-glance plan.

4.6 Closing Remark

A disciplined hybrid built on *feasibility-first repair*, targeted operator selection, and SA acceptance delivers both exceptional performance (47.9–67.4% improvements, CV $<$ 10%) and exceptional reliability across diverse problem scales. Beyond these quantitative achievements, this work provides the electric vehicle routing community with a **proven, extensible framework**—one that balances algorithmic sophistication with practical deployability. As electric fleets scale globally, such *hybrid* principled approaches to routing optimization will be essential for realizing the full operational and environmental potential of sustainable transportation. **Beyond EVRP**, the separation we advocate—*acceptance control* handled by a simple, theory-friendly SA loop and *feasibility/attribution* handled by transparent, local mechanisms—offers a template for explainable hybrids in other resource-constrained routing and scheduling problems. When compute budgets are tight and stakeholders need to understand *why* a method works, convergence/acceptance traces and feasibility-first design provide a lightweight

alternative to heavy ablation campaigns

References

A

• Aarts, Emile and Jan Korst (1989). *Simulated Annealing and Boltzmann Machines: A Stochastic Approach to Combinatorial Optimization and Neural Computing*. New York: John Wiley & Sons.

• Archetti, Claudia and M. Grazia Speranza (2014). "A Survey on Matheuristics for Routing Problems". *EURO Journal on Computational Optimization*, Vol. 2, No. 4, pp. 223–246.

B

• Bai, Ruibin, Jiawei Li, Tianyu Liang, Kexin Li, Jiahuan Yan, Wenjun Li, Tal Raviv, and Rong Qu (2023). "A review on the electric vehicle routing problems: Variants and algorithms". *Frontiers of Engineering Management*, Vol. 10, No. 2, pp. 370–389.

• Bräysy, Olli and Michel Gendreau (2005). "Vehicle Routing Problem with Time Windows, Part I: Route Construction and Local Search Algorithms". *Transportation Science*, Vol. 39, No. 1, pp. 104–118.

• Burke, Edmund K., Michel Gendreau, Matthew Hyde, Graham Kendall, Gabriela Ochoa, Ender Özcan, and Rong Qu (2013). "Hyper-Heuristics: A Survey of the State of the Art". *Journal of the Operational Research Society*, Vol. 64, No. 12, pp. 1695–1724.

C

• Cordeau, Jean-François, Michel Gendreau, Gilbert Laporte, Jean-Yves Potvin, and Frédéric Semet (2002). "A Guide to Vehicle Routing Heuristics". *Journal of the Operational Research Society*, Vol. 53, No. 5, pp. 512–522.

E

• Erdelić, Tomislav and Tonći Carić (2019). "A Survey on the Electric Vehicle Routing Problem: Variants and Solution Approaches". *Journal of Advanced Transportation*, Vol. 2019, Article ID 5075671.

F

• Felipe, Ángel, María Teresa Ortuño, Gregorio Righini, and Gregorio Tirado (2014). "A heuristic approach for the green vehicle routing problem with multiple technologies and partial recharges". *Transportation Research Part E: Logistics*

and Transportation Review, Vol. 71, pp. 111–128.

• Fialho, Álvaro, Luís Da Costa, Marc Schoenauer, and Michèle Sebag (2010). "Analyzing bandit-based adaptive operator selection mechanisms". *Annals of Mathematics and Artificial Intelligence*, Vol. 60, No. 1-2, pp. 25–64.

G

• Gendreau, Michel and Jean-Yves Potvin (2010). *Handbook of Metaheuristics*. Second Edition. Boston: Springer.

• Glover, Fred (1989). "Tabu Search—Part I". *ORSA Journal on Computing*, Vol. 1, No. 3, pp. 190–206.

• Glover, Fred and Manuel Laguna (2000). "Fundamentals of Scatter Search and Path Relinking". *Control and Cybernetics*, Vol. 29, No. 3, pp. 653–684.

• Goeke, Dominik and Michael Schneider (2015). "Routing a mixed fleet of electric and conventional vehicles". *European Journal of Operational Research*, Vol. 245, No. 1, pp. 81–99.

H

• Hansen, Pierre and Nenad Mladenović (2001). "Variable Neighborhood Search: Principles and Applications". *European Journal of Operational Research*, Vol. 130, No. 3, pp. 449–467.

• Hiermann, Gerhard, Jakob Puchinger, Stefan Ropke, and Richard F. Hartl (2016). "The electric fleet size and mix vehicle routing problem with time windows and recharging stations". *European Journal of Operational Research*, Vol. 252, No. 3, pp. 995–1018.

J

• Jeong, Ilkyeong, Kyungsik Lee, and Jong-Hyeok Park (2024). "Electric vehicle routing problem with energy consumption uncertainty: A two-stage robust optimization approach". *Transportation Research Part D: Transport and Environment*, Vol. 128, Article 104089.

K

• Keskin, Merve and Bülent Çatay (2016). "Partial Recharge Strategies for the Electric Vehicle Routing Problem with Time Windows". *Transportation Research Part C: Emerging Technologies*, Vol. 65, pp. 111–127.

• Keskin, Merve, Bülent Çatay, and Gilbert Laporte (2021). "A simulation-based heuristic for the electric vehicle routing problem with time windows and stochastic waiting times at charging stations". *Computers & Operations Research*, Vol. 125, Article 105060.

• Kirkpatrick, Scott, C. Daniel Gelatt, and Mario P. Vecchi (1983). "Optimization by Simulated Annealing". *Science*, Vol. 220, No. 4598, pp. 671–680.

L

• Li, Lianbo, Wenjian Luo, and Xin Wang (2019). "Multi-armed bandit-based hyper-heuristics for combinatorial optimization problems". *Neurocomputing*, Vol. 334, pp. 132–142.

• Lin, Chinho, K.L. Choy, G.T.S. Ho, S.H. Chung, and H.Y. Lam (2014). "Survey of Green Vehicle Routing Problem: Past and Future Trends". *Expert Systems with Applications*, Vol. 41, No. 4, pp. 1118–1138.

M

• Macrina, Giusy, Luigi Di Puglia Pugliese, Francesca Guerriero, and Gilbert Laporte (2019). "The green mixed fleet vehicle routing problem with partial battery recharging and time windows". *Computers & Operations Research*, Vol. 101, pp. 183–199.

• Mavrovouniotis, Michalis, Christos Menelaou, Stelios Timotheou, Georgios Ellinas, Christos Panayiotou, and Marios Polycarpou (2020). "Benchmark Set for the IEEE WCCI-2020 Competition on Evolutionary Computation for the Electric Vehicle Routing Problem". In: *2020 IEEE Congress on Evolutionary Computation (CEC)*. IEEE, pp. 1–8.

• Metropolis, Nicholas, Arianna W. Rosenbluth, Marshall N. Rosenbluth, Augusta H. Teller, and Edward Teller (1953). "Equation of State Calculations by Fast Computing Machines". *The Journal of Chemical Physics*, Vol. 21, No. 6, pp. 1087–1092.

• Mladenović, Nenad and Pierre Hansen (1997). "Variable Neighborhood Search". *Computers & Operations Research*, Vol. 24, No. 11, pp. 1097–1100.

• Montoya, Alexander, Christoph Guéret, Jorge E. Mendoza, and Juan G. Villegas (2017). "The Electric Vehicle Routing Problem with Nonlinear Charging Function". *Transportation Research Part B: Methodological*, Vol. 103, pp. 87–110.

P

• Pelletier, Sam, Ola Jabali, and Gilbert Laporte (2016). "Goods distribution with electric vehicles: Review and research perspectives". *Transportation Science*, Vol. 50, No. 1, pp. 3–22.

• Pisinger, David and Stefan Ropke (2019). "Large Neighborhood Search". In: Michel Gendreau and Jean-Yves Potvin (eds.). *Handbook of Metaheuristics.*

Third Edition. Cham: Springer International Publishing, pp. 99–127.

• Puchinger, Jakob and Günther R. Raidl (2005). "Combining Metaheuristics and Exact Algorithms in Combinatorial Optimization: A Survey and Classification". In: *International Work-Conference on Artificial Neural Networks*. Berlin: Springer, pp. 41–53.

R

• Rodríguez-Esparza, Enrique, Antonio D. Masegosa, Enrique Onieva, David Ramos, and Pedro López-García (2024). "A New Hyper-Heuristic Based on Adaptive Simulated Annealing and Reinforcement Learning for the Capacitated Electric Vehicle Routing Problem". *Expert Systems with Applications*, Vol. 252, Article 124190.

• Ropke, Stefan and David Pisinger (2006). "An Adaptive Large Neighborhood Search Heuristic for the Pickup and Delivery Problem with Time Windows". *Transportation Science*, Vol. 40, No. 4, pp. 455–472.

S

• Schiffer, Maximilian and Grit Walther (2017). "The electric location routing problem with time windows and partial recharging". *European Journal of Operational Research*, Vol. 260, No. 3, pp. 995–1013.

• Schneider, Michael, Andreas Stenger, and Dominik Goeke (2014). "The Electric Vehicle-Routing Problem with Time Windows and Recharging stations". *Transportation Science*, Vol. 48, No. 4, pp. 500–520.

• Shaw, Paul (1998). "Using Constraint Programming and Local Search Methods to Solve Vehicle Routing Problems". In: *International Conference on Principles and Practice of Constraint Programming*. Berlin: Springer, pp. 417–431.

T

• Taillard, Éric, Philippe Badeau, Michel Gendreau, Francois Guertin, and Jean-Yves Potvin (1997). "A Tabu Search Heuristic for the Vehicle Routing Problem with Soft Time Windows". *Transportation Science*, Vol. 31, No. 2, pp. 170–186.

V

• Van Laarhoven, Peter J.M. and Emile H.L. Aarts (1987). *Simulated Annealing: Theory and Applications*. Dordrecht: Springer.

• Vidal, Thibaut, Teodor Gabriel Crainic, Michel Gendreau, and Christian Prins (2013). "Heuristics for Multi-Attribute Vehicle Routing Problems: A Survey and Synthesis". *European Journal of Operational Research*, Vol. 231, No. 1,

pp. 1–21.

Z

• Zhang, Shaowei, Yongqi Chen, and Weishan Zhang (2019). "A novel location-routing problem in electric vehicle transportation with heterogeneous fleet". *Transportation Research Part C: Emerging Technologies*, Vol. 100, pp. 157–172.